



HAL
open science

pXRF Data Evaluation Methodology for On-Site Analysis of Precious Artifacts: Cobalt Used in the Blue Decoration of Qing Dynasty Overglazed Porcelain Enameled at Customs District (Guangzhou), Jingdezhen and Zaobanchu (Beijing) Workshops

Philippe Colomban, Gulsu Simsek Franci, Michele Gironda, Pauline d'Abrigeon, Anne-Claire Schumacher

► To cite this version:

Philippe Colomban, Gulsu Simsek Franci, Michele Gironda, Pauline d'Abrigeon, Anne-Claire Schumacher. pXRF Data Evaluation Methodology for On-Site Analysis of Precious Artifacts: Cobalt Used in the Blue Decoration of Qing Dynasty Overglazed Porcelain Enameled at Customs District (Guangzhou), Jingdezhen and Zaobanchu (Beijing) Workshops. *Heritage*, 2022, 5 (3), pp.1752-1778. 10.3390/heritage5030091 . hal-03740083

HAL Id: hal-03740083

<https://hal.science/hal-03740083v1>

Submitted on 10 Mar 2024

HAL is a multi-disciplinary open access archive for the deposit and dissemination of scientific research documents, whether they are published or not. The documents may come from teaching and research institutions in France or abroad, or from public or private research centers.

L'archive ouverte pluridisciplinaire **HAL**, est destinée au dépôt et à la diffusion de documents scientifiques de niveau recherche, publiés ou non, émanant des établissements d'enseignement et de recherche français ou étrangers, des laboratoires publics ou privés.



Distributed under a Creative Commons Attribution 4.0 International License

Article

pXRF Data Evaluation Methodology for On-Site Analysis of Precious Artifacts: Cobalt Used in the Blue Decoration of Qing Dynasty Overglazed Porcelain Enamelled at Customs District (Guangzhou), Jingdezhen and Zaobanchu (Beijing) Workshops

Philippe Colomban ^{1,*}, Gulsu Simsek Franci ², Michele Gironda ³, Pauline d'Abrigeon ⁴
and Anne-Claire Schumacher ⁵

¹ Sorbonne Université, CNRS, MONARIS UMR8233, 4 Place Jussieu, 75005 Paris, France

² Surface Science and Technology Center (KUYTAM), College of Sciences, Koç University, Rumelifeneri Campus, Sariyer, Istanbul 34450, Turkey; gusimsek@ku.edu.tr

³ XGLab S.R.L.—Bruker, 23 Via Conte Rosso, 20134 Milan, Italy; michele.gironda@bruker.com

⁴ Fondation Baur, Musée des Arts d'Extrême-Orient, Rue Munier-Romilly 8, 1206 Geneva, Switzerland; pdabrigeon@fondationbaur.ch

⁵ Ariana Museum, Av. de la Paix 10, 1202 Geneva, Switzerland; anne-claire.schumacher@ville-ge.ch

* Correspondence: philippe.colomban@sorbonne-universite.fr



Citation: Colomban, P.; Simsek Franci, G.; Gironda, M.; d'Abrigeon, P.; Schumacher, A.-C. pXRF Data Evaluation Methodology for On-Site Analysis of Precious Artifacts: Cobalt Used in the Blue Decoration of Qing Dynasty Overglazed Porcelain Enamelled at Customs District (Guangzhou), Jingdezhen and Zaobanchu (Beijing) Workshops. *Heritage* **2022**, *5*, 1752–1778. <https://doi.org/10.3390/heritage5030091>

Academic Editor:
Artemios Oikonomou

Received: 15 June 2022

Accepted: 15 July 2022

Published: 20 July 2022

Publisher's Note: MDPI stays neutral with regard to jurisdictional claims in published maps and institutional affiliations.



Copyright: © 2022 by the authors. Licensee MDPI, Basel, Switzerland. This article is an open access article distributed under the terms and conditions of the Creative Commons Attribution (CC BY) license (<https://creativecommons.org/licenses/by/4.0/>).

Abstract: In a noninvasive determination, Raman and XRF analyses showed the possibility of identifying specific phases and elements characteristic of the use of recipes and ingredients imported from Europe, according to the information documented in Chinese and European archives. Two sets of objects, supposed to have been produced during the Qing Dynasty (1662–1912) at the Forbidden City ('imperial bowls' of the Baur Foundation, Geneva) and in the customs district of Guangzhou (Musée Ariana, Geneva), were analyzed with pXRF and also for some objects with Raman microspectroscopy also on-site. The heterogeneity of the colored zones, in three spatial directions, requires the development of a new methodology. We focused particular attention on the cobalt used in the colored areas and marks, drawn either on the body layer (standard underglaze) or on the glaze itself (overglaze). Comparison is made with previous data on Chinese and Vietnamese porcelains from the Yuan (1271–1368) and Ming Dynasty (1368–1644) periods. Combined data for objects attributed to Guangzhou from the Kangxi and Yongzheng periods indicates the use of the same raw materials containing cobalt, associated with arsenic, nickel, zinc, copper and bismuth, according to the European sources. Similarity of the glaze composition and impurities promotes the production of the glazed body with the same raw materials as those used at Jingdezhen. A consistent shift in data for Qianlong style items, which are significantly richer in manganese, is compatible with their partial mixing with Asian cobalt. The deliberate selection of conflicting objects—namely, examples belonging to the other places of production or different periods—are well-observed outside the 'Guangzhou' cluster. Some artifacts have anachronistic purity characteristics that support a production after ca. 1850. For instance, two objects on which certain attributions had been made concerning the stylistic analysis are definitive examples of ceramics using a refined 'cobalt', and therefore now may be assigned to the later production period of the first half of the 19th century.

Keywords: imperial porcelain; overglaze; underglaze; Qing Dynasty; blue; cobalt; XRF; mark; arsenic; authentication

1. Introduction

The transfer of knowledge and the production of everyday objects in an economically more favorable region because of the availability of heavy raw materials, expertise and inexpensive labor, which characterize the globalization of the economy, are frequent in the 20th and 21st centuries. Correspondence from the Jesuits in residence at the Forbidden City,

information extracted from the Chinese archives [1–9] and envoys of Louis XIV the French King to the court of the Chinese Emperor Kangxi (1662–1722) indicate the importation of ingredients from Europe to China. The participation of the Jesuits is reported in the extension of the color range of enamels from about six colors to a variation, allowing the possibility of mixing to obtain a range of nearly 30 shades. This helped to produce enamel decoration comparable to what was obtained in oil painting, as made by European craftsmen for more than a century [8–13]. The assumption is that the primary enamel productions, first on glass, then on metal ware, and porcelain ‘blanks’ produced in the imperial kilns of Jingdezhen, were made at the glass production workshop established by Kilian Stumpf in 1696 [14]. It also appears that during the first decade of the 18th century, workshops were set up in the customs district of Guangzhou (‘Canton’), a place where Westerners were able to stay and trade with China to produce enameled objects for the Imperial Court and for export (particularly armorial porcelain table services) [9,15–21]. The shades obtained with the imported recipes/ingredients are blue, white, new shades of green and colors ranging from pink to purple [6].

Let us briefly recall what we know about the motivation and advantages of using European recipes and ingredients. The cobalt-rich raw material used by potters during the Ming period and most of the Kangxi reign is derived from primary Asian geological sites [22,23]. It contains an equivalent quantity of other transition metals (iron, manganese, etc.) [23], which imposes a firing under strict reducing conditions to obtain a correct blue color [23–27]. However, an oxidizing atmosphere leads to ‘dirty,’ blackish, or greenish hues and black spots [21,23,26,27]. On the contrary, European cobalt raw material (the ‘smalt’, a potassium glass obtained from ‘saffre’ issued from silver and/or bismuth production slags) [23] contains arsenic, which gives a white opacification magnifying the blue color by the reaction with the lead-based silicate matrix of the enamel. The cobalt–arsenic association in Kangxi productions is well-supported [12–14,21,23–25,28,29] and comparable to that observed in European enamel objects, regardless of the type of substrate, metal, glass or porcelain [10,11,30–34]. Indeed, the elements associated with cobalt depend not only on the ores but also on their processing, which means that the number of associated elements of the same source will vary in the final product [23].

The opacification in white was traditionally obtained in China by the use of fluorite (CaF_2) [10,14,25,35]. The use of lead arsenates with variable and complex compositions [11–13,21,23,25–31] is also considered a Western contribution. The green color traditionally obtained by dissolution of Cu^{2+} ions in the silicate glass network allows only two shades, namely a ‘jade’ green if the flux is lead-rich and turquoise if the glass is alkaline. The European technique for obtaining different shades of green by dispersing a yellow pigment (‘pure’ tin yellow or, more widely, the different Naples yellows with a complex pyrochlore structure and composition) in a blue-colored matrix by cobalt ions is much more versatile [11,30–34,36–43]. Shades of pink to purple are obtained by the dispersion of colloidal gold prepared by dissolving gold in aqua regia and the precipitation of gold in the form of nanoparticles by a redox reaction with the addition of tin (purple of Cassius) or arsenic (Perrot’s red), the color depending on the size of the nanoparticles then dispersed in the glassy silicate [11,21,34,35,44,45].

In this paper, we present X-ray Fluorescence (XRF) analyses of the areas colored in blue (decoration and reign marks) carried out on-site. The artifacts studied here are six bowls potentially assumed to be made for the Emperor, some of which are assumed to be made at the workshop of the Forbidden City (Zaobanchu, 造辦處, Beijing, named *huafalang* 畫琺瑯 or *falangcai* 琺瑯彩), or in the imperial kiln of Jingdezhen, named *yangcai* 洋彩, belonging to the Baur Foundation’s collection, and twelve porcelains assumed to be made at the workshops in Guangzhou (Canton) and/or Jingdezhen, in addition to two artifacts assigned to Arita (Japan) and Meissen (Saxony), all belonging to the Ariana Museum collections. The bowls were also analyzed on-site by Raman microspectroscopy. Most of the artifacts are assigned to the Kangxi 康熙 (1661–1722) and Yongzheng 雍正 (1722–1735) reigns. The objective is to identify the elements associated with cobalt by

comparing the measurements carried out on the blue areas and those that are not colored to appreciate the perturbation arising from the silicate matrix of the enamel. Indeed, a determination of composition is impossible due to the variable penetration of X-rays according to the energy of elements (see further) and low—and variable—thickness of the colored layer and the intrinsic variation in the distribution of the coloring agents imposed by the production of a complex decoration. The contents of cobalt and associated elements is compared with our previous studies of Vietnamese and Chinese porcelains of different periods and origins [23,27,46–48]. This study is devoted to the blue color because previous works [23,28,29,36,47,49] have shown that due to the very different geological context of the cobalt mines then being exploited in Europe and Asia, the mobile techniques of Raman and XRF analyses identified the different types of cobalt sources from the minor, trace elements associated with cobalt and the resulting phases which formed by reaction with the silicate matrix of the enamel. For example, the cobalt sources of Asian origin are very rich in manganese and iron while those from Europe contain a lot of arsenic [23,26,27,29,49]. It is commonly accepted that the porcelain paste was prepared and fired in Jingdezhen, in ‘official’ (Imperial) or private kilns. Based on the pXRF and Raman measurements, the location of the enameling places is discussed. Some criteria commonly used to distinguish the enameled productions in Jingdezhen, Guangzhou or Beijing (Forbidden City), based on visual criteria, remain open for debate. The analyses presented here support or challenge the attribution by assigning production sites of some of the artifacts in question.

2. Materials and Methods

2.1. Portable X-ray Fluorescence Spectroscopy (pXRF)

X-Ray Fluorescence analysis was performed on-site using a portable ELIO instrument (ELIO, Bruker, Berlin, Germany) as described in previous studies [11,25,50]. The set-up viewed in Figure 1a includes a miniature X-ray tube system with a Rh anode (max voltage of 50 kV, max current of 0.2 mA, and a 1 mm² collimator), and a large area Silicon Drift Detector (SDD, 50 mm² active areas) (ELIO, Bruker, Berlin, Germany) with an energy resolution of <140 eV for Mn K α , an energy range of detection from 0.9 keV to 42 keV (from 1.3 keV in air) and a maximum count rate of 5.6×10^5 cps. Depending on the object, the measurement is carried out by positioning the instrument on the top (Figure 1a) or on the side (Figure 1b). A perfect perpendicularity to the area being measured is needed. Focusing is controlled by the laser.

Measurements were carried out in the point mode with an acquisition time of 120 s, using a tube voltage of 50 kV and a current of 80 μ A. No filter was used between the X-ray tube and the sample. During the analysis, the working distance between the sample and detector was around 15 mm, and the distance between the instrument front and artifact was about 10 mm. The signal-to-noise ratio (SNR) of the spectral signals was optimized with the set-up parameters described above. The analysis depth, defined as the thickness of the top layer from which comes 90% of the fluorescence (which depends from the photon energy, type of material (atom number) and material density), is calculated using the Beer-Lambert law [51]. The thickness is estimated to be close to 6 μ m at Si K α , 170 μ m at Cu K α , 300 μ m at Au L α and 3 mm at Sn K α . Within the resolution of the pXRF instrument, the Fe K β peak and the Co K α peak are located in the same energy range. To identify visually the presence of Co in enamel spectrum (except when cobalt is present in traces), we can use the information obtained by looking at the Fe K α /Fe K β ratios. In the absence of cobalt, the relative intensity between Fe K α and Fe K β peaks is about 6/1. Cobalt is then obvious if the superimposed peaks of Co K α and Fe K β exhibit a stronger intensity than that expected from the above ratio.



Figure 1. View of the XRF analysis set-up, the measurement can be made from top (a) or side (b), the orientation of the instrument being variable and the XY displacement motorized and computer-controlled; (c,d) views of the Raman analysis, from the decoration or the mark by using a 50× microscope objective. See references [10–13,50] for more details about the mobile Raman set-up.

2.2. Processing of XRF Data

After recording the raw data with ELIO, the Spectra (the so-called .spx) files are open in the Artax 7.4.0.0 (Bruker, AXS GmbH, Karlsruhe, Germany) software. For the data treatment process, the studied objects are considered infinitely thick samples. Before evaluating the analysis data, all the spectra are imported, and a new method file is created via the ‘Method Editor’ of Artax for the applied voltage 50 kV and current 80 μ A. The major (e.g., K, Ca), minor (e.g., Fe, Ti, Co) and trace elements (e.g., Ag, Bi, As) are added in the periodic table. For the correction, escape and background options are selected in the Method Editor. Additionally, 10 cycles of iteration were selected starting from 0.5 keV to 45 keV. The deconvolution method, Bayes, was applied for the export of results. The net area under each peak was calculated at the characteristic energy of each element selected in the periodic table, and the counts of the major, minor, and trace elements were plotted in the binary/ternary scattering plots drawn with the software Statistica 13.5.0.17 (TIBCO Software Inc., Palo Alto, CA, USA). For the comparison of these data with the older measurements, especially those carried out with Bruker instruments but using its different portable models, a normalization procedure was applied by taking the ratio of the major (K, Ca), minor (Mn, Ni, Fe, Cu, As) and trace elements (Ag, As, Bi) with the number of XRF photons derived from the elastic peak of the X-ray tube of rhodium. We also normalized

the data to the major element found in the matrix that we analyzed; for instance, Si in the enamel in addition to the calculation of the ratios of the net number of XRF photons of the elements (K, Mn, As, Ni, Fe, Cu, Zn Bi, Ag) versus cobalt (coloring element for blue).

For the interpretation of the results with a statistical approach, a hierarchical Euclidian clustering diagram was drawn by using the data obtained from the XRF photons of Pb, K, Mn and As with the software Statistica (Statsoft-TIBCO Inc., Palo Alto, CA, USA).

2.3. Raman Microspectroscopy

Raman analyses were carried out in the exhibition room of the Foundation Baur museum (Figure 1b) with a mobile HE532 Raman set-up (HORIBA Scientific Jobin-Yvon, Longjumeau, France) as extensively described in the references [10–13]. For each colored area in the objects concerned, at least three Raman spectra were recorded to check the representativeness of the collected data on a statistical basis. The reliability of the Raman spectrum starts above 80 cm^{-1} , but a flat spectral background is only obtained over 500 cm^{-1} . A $50\times$ (17 mm long working distance, Nikon France SAS, Champigny-sur-Marne, France) objective was used (surface spot waist $\sim 2\text{--}4\ \mu\text{m}$; in-depth $<5\text{--}10\ \mu\text{m}$, the values varying with the color) by positioning it perpendicular to the sample surface, which allows the recording of spectra which are not affected or only minimally affected by the sublayers and/or the silicate matrix if the grains are bigger than $\sim 5\ \mu\text{m}$. Obviously, the power of illumination at the sample should be minimal ($\sim <1\text{ mW}$) for dark-colored areas due to the absorption of light, although up to 10 mW is required for the examination of light-colored or colorless areas of the enamels.

2.4. Objects Studied

Tables 1 and 2 list the studied objects presented in Figure 2. The XRF measurements are carried out on the blue area shown in the Figures as well as on an area of the nearest transparent glassy cover (appearing ‘white’). The artifacts were selected to represent the variety of decorations using the color blue among Qing Dynasty porcelain, from the Kangxi to the Qianlong reigns. Original attributions are given in the table, but they remain debatable. The Baur Foundation, Museum of Far Eastern Art in Geneva, possesses a remarkable collection of imperial enameled porcelain dating from the late 17th and early 18th centuries, from the reigns of Kangxi, Yongzheng and Qianlong 乾隆 (1736–1795).

Table 1. Non-Chinese (two) and Chinese (eleven) artifacts from Ariana Museum collection and their main characteristics (H: height; L: width).

Artefact	Inventory Number	Period	Dimension (cm)	Expected Place of Enameling (characteristics)	Analyzed Area
Soap box	AR 9168	19th century	H: 8 L: 13.8 l: 10.5	Canton?	Women coats
Plate	AR 4530	Yongzheng, ca. 1730	H: 2.8 D: 22.5	Canton?	Flower, men coats
Plate	AR 4608	Yongzheng, ca. 1730	H: 5 D: 35.3	Canton or Jingdezhen?	Box close to yellow vase mark
Cup saucer	AR 10091	Yongzheng, 1723–1735	H: 4.5 D: 11.7	Canton?	Men coats
Plate	AR 2007-196	Yongzheng, 1723–1735	H:3.2 D: 20.7	Canton or Jungdezhen? (Ruby-back)	Vase
Plate	AR 2007-213–2	Yongzheng, 1723–1735	H:3.7 D: 21	Canton?	Vase
Plate	AR 2007-202	Yongzheng, 1723–1735	H: 3.3 D: 21	Canton or Jingdezhen? 7 borders decor, ruby back	Vase
Plate	AR 3646	Qianlong, ca. 1745	H:4 D: 22.8	Canton? Pierre-Paul Rubens inspired decor	Mountain ridge

Table 1. *Cont.*

Artefact	Inventory Number	Period	Dimension (cm)	Expected Place of Enameling (characteristics)	Analyzed Area
Plate	AR 4601	Qianlong, ca. 1740	H: 2.5 D: 22.3	Canton? (‘ <i>Xixiang ji</i> ’ story décor)	Tree branch
Plate	AR 10818	Qianlong, ca. 1735–1740	H: 4.5 D: 36	Meissen style	Mountain summit
Dish	AR 3680	Qianlong, ca. 1740–1743	H: 2.8 D: 22.8	Armorial decoration (Elias Guillot coat-of-arms, Holland), Canton?	Marli, Coat-of-arms, Helmet

Table 2. Artifacts from the Foundation Baur Collection and main characteristics (the last three digits of the inventory number are used in the text following the letter A).

Artifact	Inventory Number	Period	Reign Mark	Dimension	Analyzed Blue Spot	Analyzed Glaze	Analyzed Body
bowl	CB.CC.1936.677	but probably later period	Kangxi reign mark in red	D. 14.5; H. 7.4	background	yes	no
bowl	CB.CC.1932.613	Kangxi	Kangxi reign mark in cobalt blue	D. 12.5	flower, light blue, mark	close to flower close to mark	yes
bowl	CB.CC.1950.672	Kangxi	Kangxi reign mark in cobalt blue	D. 12.5; H. 6.5	flower mark	close to mark	yes
bowl	CB.CC.1937.615	Yongzheng	Yongzheng reign mark in cobalt	D. 11	flower, mark	close to mark	yes
bowl	CB.CC.1930.616	maybe later date	Yongzheng reign mark	D. 9.3	blue (background), mark	close to mark	no
bowl	CB.CC.1930.630	Daoguang 1821–1850	Daoguang reign mark in cobalt blue	D.18.5	flower, mark	close to mark	no
dish	CB.CC.1935.608	Qianlong 1736–1795	Qianlong reign mark in cobalt blue	D. 17.4	Men coats (XRF mapping)	yes	no

Reign marks, by design, usually feature the name of a specific reign period and then, from the Ming Dynasty onward, also the name of the dynasty. Kangxi-period imperial bowls bearing the Kangxi yuzhi mark 康熙御制 were, when first published, the subject of controversy over their authenticity [52]. In an article published in 1969 by Harry Garner [53], all these marks were given as false based on the Jesuit archives uncovered a few years earlier by George Loehr [54]. Since then, Harry Garner’s opinion has been largely disproved, and the latest Foundation catalogues have revised these attributions [55]. It is since commonly assumed that pieces with an underglaze cobalt blue were painted at Jingdezhen for the court, while the reign mark with overglaze reign marks were painted in the imperial workshop of the Forbidden City [56].

The study of marks and their authenticity are the subject of research [56,57], but the study of their composition has not been undertaken in a global manner. Chinese ‘false’ marks were even applied to Japanese porcelains [58]. Some pieces remain problematic, however, their form, style and even color contrast with much more refined works from the same period. The Kangxi period, during which these new colors were developed, was a time of experimentation, and it should therefore be emphasized that the style and quality of the glazes may vary. Scientific analysis was therefore considered as a means of eliminating those pieces of which the enamel composition was definitely of a later date.



Figure 2. Cont.



Figure 2. Top, view of imperial bowls and a dish with European-inspired decoration (right dish A608, Baur Foundation Collection, see Table 2); bottom, objects from the Ariana Museum Collection (See Table 1). Zooms on the analyzed blue areas are given.

Alongside these pieces produced for the emperor either in Jingdezhen or in the imperial workshops in the Forbidden City are the pieces produced specifically for export (*waixiao ci* 外銷瓷). These were made in private kilns in Jingdezhen, sometimes painted on the spot, sometimes sent undecorated to Guangzhou (Canton) [18–21,24,59,60] where they were painted in local enameling workshops (these works are then called *Guangcai* 廣彩). Canton’s enamel workshops came into being in the early decades of the 18th century. Their location in this port, which was then the only place where Europeans were allowed to trade with China, made it easier to respond to specific orders from Europe [15–21]. For a long time, the production of painted decoration in Canton tended to be underestimated in comparison with that of Jingdezhen. However, historians have challenged this assumption in recent years, arguing that the Canton workshops achieved a very high level of mastery of painted enamel very early on [59,60]. This position, supported by both archival sources and stylistic analyses, has made the differentiation of the two production sites more complex. Therefore, the present article aims to contribute to this debate by publishing the results of physicochemical analysis on a group of works dating from the 18th and early 19th centuries with the hope of bringing to light new hypotheses on possible differences in the composition of enamels between the two production sites.

The Ariana Museum possesses a large number of pieces of various periods and countries, in particular characteristic of export porcelain from the Yongzheng and Qianlong periods, as well as a set of enamels commonly accepted as being painted in Canton in the 19th century, from which samples have been taken [61,62]. For comparison, two foreign pieces were added, a Japanese Arita porcelain dated from the very end of the 17th century [63–69], painted with enamels on glaze in the Kakiemon style, and work from the Meissen factory dating from the mid-18th century. The integration in the same study of pieces from the imperial workshops and pieces made for export would also allow one intended to compare the techniques used on the same color and the possible correspondence of compositions from one site to another.

Data of previous XRF studies of Vietnamese (excavations from Chù Dau and other sites from the Hong river, excavated from the kiln sites [26,46] or from the Cù Lao Cham shipwreck, Hoi-An, [46] Vietnam, excavated from Qalhat, Sultanate of Oman [27]) and China (excavated from Qalhat [27], collected from the Vietnamese site (Hoa Lu) and Blue Print Collection [47,48]) artifacts dated from the 14th to 16th centuries, are used for comparison (more than 30 samples). This comparison is used to identify the discrepancy of the different elements associated with the blue color and the changes incurred with time.

3. Results

3.1. Comparison Paste–Glaze–Overglaze

For a more didactic comparison of the analyses, we first consider the appearance of the pXRF spectra and their visually obvious characteristics. A more in-depth analysis is then made from the calculations with the Artax process. The XRF spectra is in the 0.1 to 15 keV energy range, where the characteristic peaks of the $K\alpha$ (and $K\beta$) transitions of the elements K and Ca appear for the (earth) alkaline flux, transition metals (in increasing order of energies: Ti, Mn, Fe, Co, Ni, Cu, and Zn) as well as the $L\alpha$, $L\beta$ and $L\gamma$ strong transitions of lead (Pb). Additional small lead peaks of additional transitions can be also be present. To these are added the peaks of rubidium (Rb), yttrium (Yb), strontium (Sr), zirconium (Zr) and uranium (U). Strontium and rubidium are the trace elements associated with calcium and potassium (Figure 3). Zirconium is generally present in the form of zircon ($ZrSiO_4$), a very stable phase, associated with rutile/anatase/brookite (TiO_2), which are commonly found in igneous rocks and associated detrital rocks. Thus, it is obvious to distinguish a lead-containing overglaze from a flux based on potassium, calcium and sodium (the last element is not measurable by mobile XRF in the air) and from the body paste.

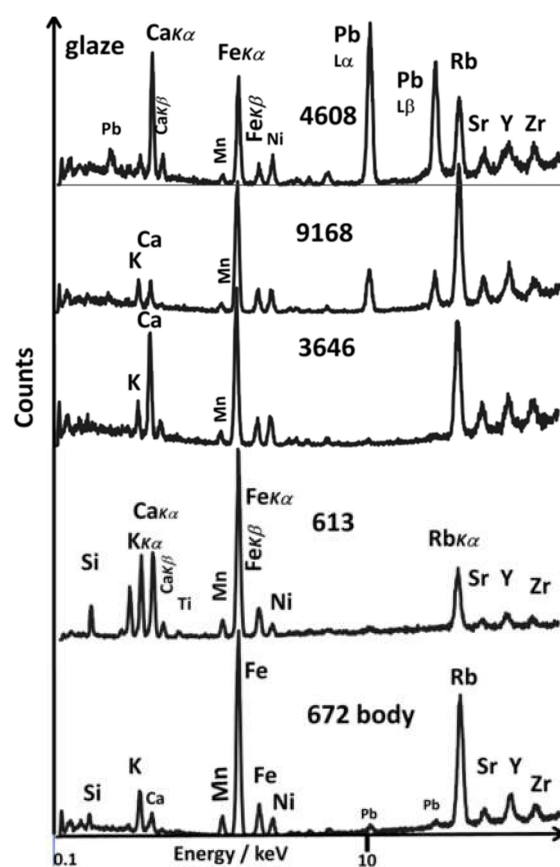


Figure 3. Comparison of XRF spectra showing the representative spectrum of porcelain body in the bottom and different type of glazes above.

The $K\beta$ peaks of the elements calcium and iron are also very visible. However, the $K\alpha$ peak of the cobalt is confused with the $K\beta$ peak of iron for the resolution of the instrument used in this study (Figure 4). Similarly, the $K\alpha$ peak of arsenic is confused with $L\alpha$ peak of lead (it can be estimated as a weak shoulder on the peak) and only the smaller As $K\beta$ peak located between the two intense peaks of lead, after a minor peak also of lead, makes it possible to evaluate without ambiguity the presence of arsenic (it is very well detected by Raman due to the high intensity of the As-O elongation mode, see further) [10–13,23,28,70]. The presence of tin and antimony is detectable in the 25–30 keV range (Figure 5), but for these elements (as for lead), the volume probed by the X-rays is deeper (e.g., 2.5 mm for Sn $K\alpha$) than the commonly observed thickness of the overglaze (100–300 μm [13,21]), and therefore the measurement is distorted by the substrate contribution (glaze and/or paste). However, for transition metals (e.g., Fe, Mn, Ni, Cu), the probed thickness (~200 to 300 μm) is similar than that of the colored layer. Only, the probed thickness of bismuth (one of the trace elements of the cobalt source) is almost equivalent to the thicker-colored layer (~300 μm), and therefore may be distorted from the presence of the substrate. For this reason, it makes no sense to want to determine ‘an enamel composition’, especially since the concentration of coloring agent varies from point to point for the creation of a complex decoration. Hence, it is necessary to evaluate the disruption of the XRF measurement of an overglaze decoration by comparing the estimated contribution of the glaze/silicate matrix on a case-by-case basis.

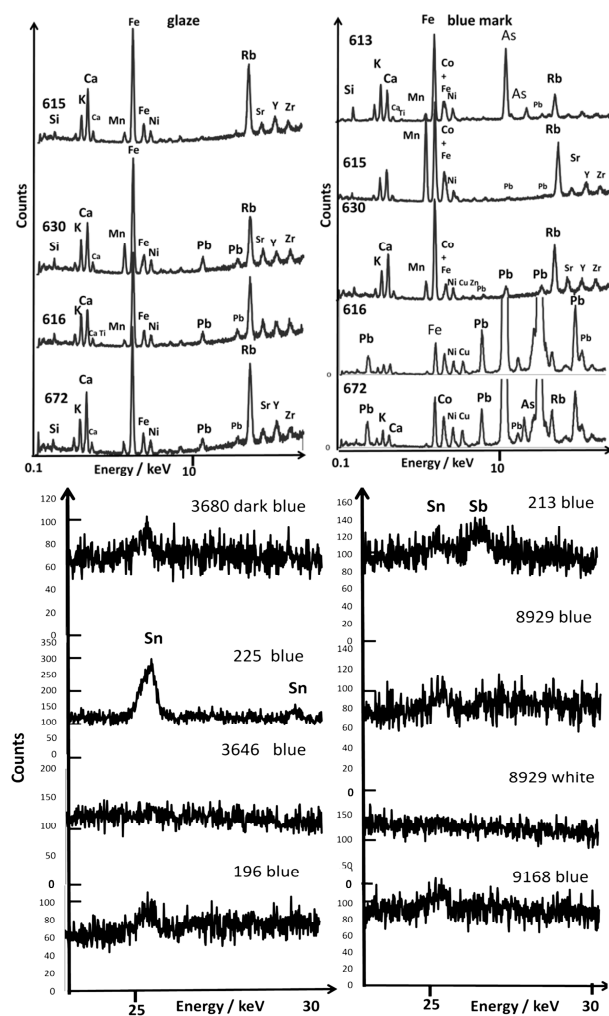


Figure 4. Comparison of pXRF spectra obtained for the different types of reign marks and associated glaze. Zoom on bottom shows the comparison of pXRF spectra in the ~20–30 keV energy range for blue and colorless examples.

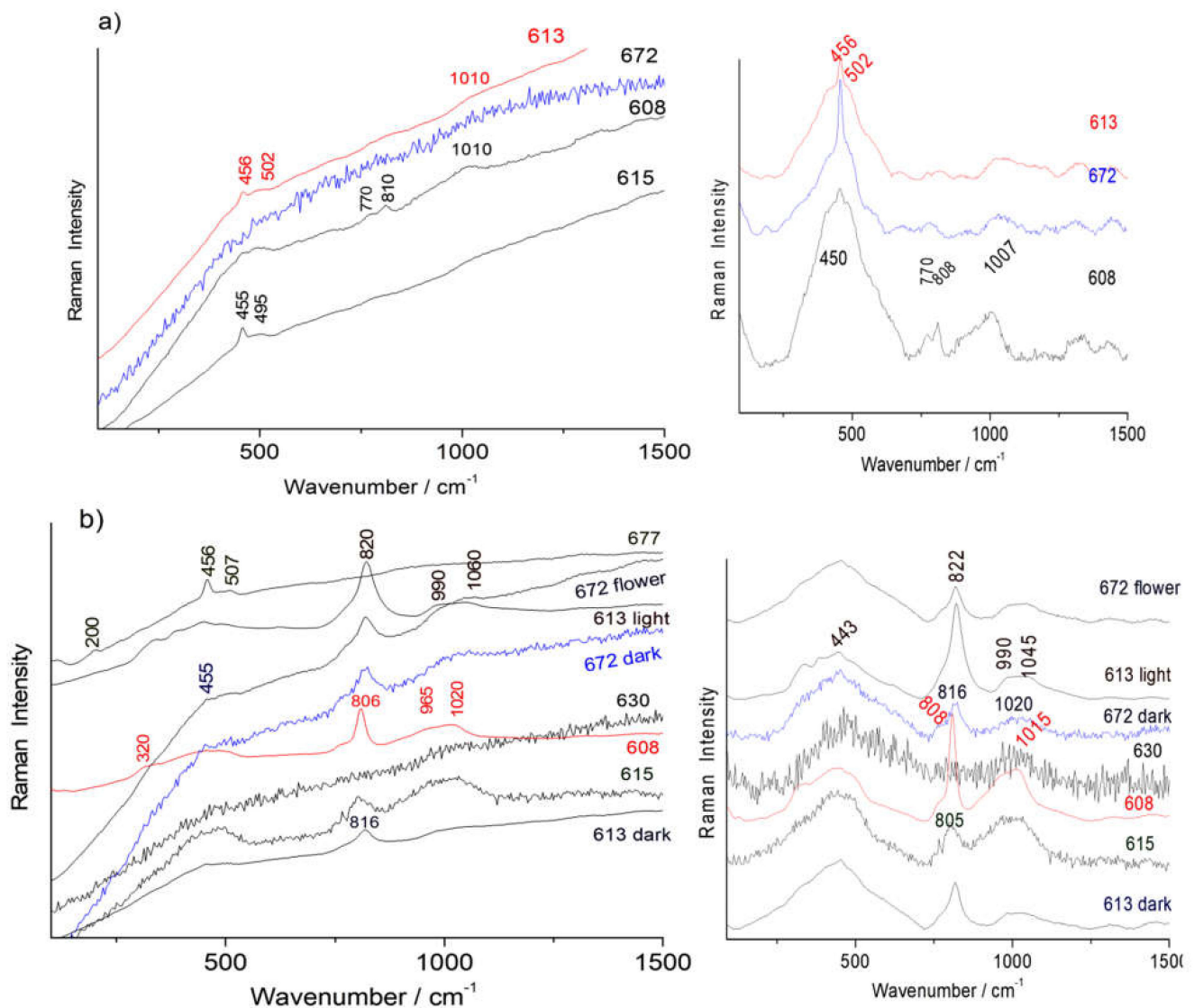


Figure 5. As-recorded Raman spectra recorded on the blue reign mark (a) and on the other focused blue areas (b) for some artifacts of Table 2 (A 677: blue background; other: decoration). On the right the spectra after baseline subtraction. Colors are used to differentiate spectra.

We now take some examples. Figure 3 compares representative spectra of a porcelain paste and different glazes. We see that the glaze is richer in calcium than the body, but two types of glazes exist as reported previously [21,71], depending on the amount of calcium. In addition, there is a contamination by lead, which remains very low (only the two main peaks are scarcely detected, for example for the artifacts AR 3646 and A 613, Figure 3). This contamination occurs during the firing of the overglaze. The oxide of lead is very volatile above ~ 850 °C, recondensing upon cooling on the surface of the whole object and reacting with the glaze surface. The release of lead by pollution from the furnace is possibly an additional cause. On the other hand, for the object AR 4608 (supposedly made according to stylistic analysis in Guangzhou during the reign of Yongzheng, ca. 1730), the intensity of the lead peak is too significant not to correspond to a voluntary addition, as seen in some export productions [21]. Thus, the glaze contains a low amount of lead oxide. The intensity of the Pb peak is much higher in the overglaze (see e.g., the spectrum of the A 616 and A 672 blue mark (over) glaze in Figure 4). The surface of the paste, in the free areas of the foot cover, also shows a slight lead pollution.

A weak peak of manganese is associated with that of iron as well as traces of nickel, Zirconium and yttrium, sometimes titanium and uranium are also detected as well as rubidium and strontium trace elements always associated with calcium and potassium.

3.2. European and Asian ‘Cobalt’

Cobalt, one of the transition metals, is a rare element, and thus the number of geological sites which allow the exploitation of minerals containing a significant amount of this element is very limited. Moreover, until the middle of the 20th century, there was only one other alternative, which allowed one to color in blue, namely a crystalline natural silicate, also known as lapis lazuli, a rare rock [23,36]. To date vanadium-doped zircon the main blue pigment is used [72]. The scarcity of cobalt has led to the recycling of blue glass since antiquity [23]. Geologically, in a simple way we can classify the cobaltiferous sites into three groups: (i) the primary sites resulting from moderate transformation of polymetallic nodules made of oxyhydroxides of transition metals, namely cobalt, iron and manganese, formed at the deep sea level; (ii) the secondary sites where hydrothermal circulations led to the precipitation of sulfides and cobalt arsenides enriched in elements such as silver and bismuth and (iii) ternary sites resulting from subsequent degradations such as evaporites from salt lakes [23,36,49]. The deposits of recent regions (geologically speaking, such as around the Himalayas) are generally of the first type, while in Europe the sites located in the old Hercynian mountains are of the second type.

For a long time, efforts have been made to identify the elements associated with cobalt, allowing the production mining to be identified [23,29,73–87]. Thus, it is considered that during the Yuan Dynasty (1271–1368) the cobalt used was mainly imported from Iran or perhaps even Europe, therefore from the second type [23,73–87], while Asian cobalts (from China, Vietnam and Malaysia/Indonesia), which are rich in Mn and Fe were used [23,26,27,29,73–87] throughout the Ming Dynasty (1368–1644). Recent works have confirmed the assertions of Chinese and European documents from the 18th century mentioning the importation of cobalt or even of ready-to-use ingredients from Europe [2,4–9,12,14,23,29]. The ‘chemical’ signature does not only depend on the material extracted from the mine but also on its subsequent treatment (grinding, washing, heating, acid treatment, etc.), depending on which element is the main one justifying the mining or a byproduct [23,85–87]. Thus, in Europe, cobalt was a byproduct of the exploitation of silver (~until the 17th century) for a long time and then of bismuth (16–17th century), obtained from the slag by the addition of potash glass (‘saffre’) to obtain various grades of ‘smalt’, before being exploited for itself (>18th century). Refining was only effective from the (middle of the) 19th century [23,85–87].

The identification of the elements with XRF and phases with Raman microspectroscopy allows the classification of the blue enamel as a function of the type of cobalt used.

3.3. Comparison of Reign Marks

The practice of imitating Song ceramics in Ming Imperial porcelain is well-established [57]. This led to the production of objects which responded to the objects from the past, including antiques, in a manner which was, to some extent, similar to copying and to the application of ‘ancient’ reign marks. Reign marks were used appropriately in most cases, but reign marks of an earlier period were applied to the objects to point out a connection with that period [57]. Production of porcelain is also seriously affected by forging. Attempts to distinguish between genuine and fake mark/porcelain were made considering the diameter and number of the bubbles in the glaze matrix close to the mark [88,89] or by the control of the very thin corroded glaze layer [90].

The objects produced for the imperial court have on their bases or on the reverse side a reign mark (Figure 2), respectively, Kangxi yu zhi 康熙御製, Yongzheng yu zhi 雍正御製, Qianlong da Qing Qianlong nian zhi 大清乾隆年製 and Daogang da Qing Daoguang nian zhi 大清道光年製 for the artifacts studied here. Figure 4 compares XRF spectra recorded on the colorless glaze with those obtained by focusing roughly on the blue reign mark line

(Figure 1d). The different part in the spectrum arises from the imperfect focusing on the blue area and that the blue color (and hence the amount of coloring Co^{2+} ions) is more or less dark. The undesired contribution of the glaze hosting Co^{2+} ions is thus variable. Some marks seem visually to be made in lead-rich overglaze (A 608, A 616, A 630, A 672). As shown in Figure 3 for lead-based enamels, the spectrum is dominated by the peaks of lead, and it is necessary to magnify the spectrum by a factor of 5 to 10 to see the peaks of the other elements. It is obvious that different types of cobalt sources are used to imprint the marks: cobalt-rich in manganese for bowl A 615 (Yongzheng reign), cobalt-rich in arsenic for bowl A 613 (Kangxi reign), cobalt with copper (A 616, Yongzheng reign) and cobalt-rich in arsenic and copper (A 672, Kangxi reign). So, we have a variety of cobalt sources that look independent of the reign mark. For an efficient comparison, we use the data in ternary scattering plots in the next paragraph, as carried out for the other objects presented in the previous studies [23].

Figure 4 also shows representative spectra in the 20–30 keV range where the characteristic pXRF peaks of tin and antimony can be compared visually. Unexpectedly, some tin and antimony are detected in the blue areas. We discuss this point further later.

3.4. Phases with Raman Identification

The Raman spectra make it possible to identify the phases (Table 3), whether amorphous (the silicate matrix constituting the enamel) or crystalline (pigments, phases forming by reaction between the molten enamel and support and residues of raw materials which have not been dissolved). The Raman spectra of the glazes of objects A 613, A 615 and A 672 show the characteristic spectrum of an alkaline/earth-alkaline glaze [91–93], i.e., a broad SiO_4 deformation mode around 490 cm^{-1} and a broad stretching mode around 1000 cm^{-1} . In addition, the main narrow mode at $\sim 455\text{ cm}^{-1}$ referring to unreacted quartz grains occurs, at a wavenumber lower than that measured for a free quartz fragment (465 cm^{-1}), as a result of the tensile stress from the bonding with the glassy silicate matrix. Exactly the same spectra (Figure 5a) are recorded when focusing on the blue lines of the blue mark for these artifacts. Thus, blue color is obtained by dissolving Co^{2+} ions in the glassy network without any formation of crystalline phases [23].

Table 3. Phases identified with Raman in the imperial bowls and a Qianlong dish with a decoration of European figures.

Artifact	Inventory Number	Assignment (Stylistic Criteria)	Analyzed Blue Spot	Phases in Glaze	Phases in Blue Area	Mark	Expected Recipes
bowl	A 677	Kangxi mark but probably later period	background	quartz vitreous silicate	quartz vitreous silicate	- (red mark)	Overglaze mark
bowl	A 613	Kangxi	flower, light blue, mark	quartz vitreous silicate lead arsenate	quartz vitreous silicate lead arsenate	quartz vitreous silicate	European-like? underglaze(?) mark
bowl	A 672	Kangxi	flower mark	quartz vitreous silicate	quartz vitreous silicate lead arsenate	quartz vitreous silicate	European? Overglaze mark
bowl	A 615	Yongzheng	flower mark	quartz vitreous silicate	quartz vitreous silicate lead arsenate	quartz vitreous silicate	Ming-like Underglaze mark
bowl	A 616	Yongzheng mark but maybe later date	blue (background) mark	not measured	not measured	not analyzed	Overglaze mark
bowl	A 630	Daoguang 1825–1850	flower mark	see for blue area	quartz vitreous silicate	quartz vitreous silicate	Ming-like Underglaze mark
dish	A 608	Qianlong	Men coat (mapping)	quartz vitreous silicate	quartz vitreous silicate lead arsenate	As traces	European? Overglaze mark

- The Raman spectra of the blue decorated areas (Figure 5b) are divided into two types:
- (i) The spectra of blue-colored areas of bowl A 677 (background) and bowl A 630 (flower) are similar to those recorded on the blue marks (A 613, A 672, A 615 bowls) with the characteristic bending peak of quartz ($\sim 455\text{ cm}^{-1}$) and glassy phase (peak between 495 and 502 cm^{-1}), representative of a glaze fired at a higher temperature with the porcelain paste. The coloring is hence obtained by dissolving the cobalt ions in the glaze, which is a traditional technique [23,33];
 - (ii) The spectra of A 608 (dish mark), A 613, A 615 and A 672 (bowls) show a stretching SiO_4 mode around $1000\text{--}1020\text{ cm}^{-1}$ with a lower wavenumber component, characteristic of the addition of lead [30–32,91–93]. The modes at ~ 780 and 815 cm^{-1} , which are characteristic of the As-O stretching mode of a lead arsenate [11–13,21,25,28,32,50], are simultaneously observed. This is consistent with a lead-based enamel promoting the precipitation of lead arsenate by the reaction between the enamel and cobalt source or a deliberate addition of arsenic to whiten the blue color, varying from dark blue to a ‘bleu celeste’ hue.

4. Elements Associated with Cobalt

The heterogeneity of the distribution of coloring agents occurs horizontally to constitute the decoration and depth due to the variations in thickness and tones of the overglaze layer. According to the energy of the characteristic peaks of the element in analysis, the probed depth will vary, leading to the use of a particular procedure to compare the ‘local compositions’ of some elements of different objects, a fortiori when the measurements are made with different instruments. In fact, the constitution of ternary diagrams from the net number of XRF photons deforms the representation compared with what a ternary diagram calculated from the compositions would give. It is similar to the transformation of a geographical map incurred by replacing the distance by the travel time; the representation is distorted, but it is possible to compare and in particular to see if the distribution of the data is spread out or clustered, defining groups. A priori, the comparison of XRF signals concerning transition metals is reliable because the depth explored by the different instruments is very comparable. The main disturbance arises from the layer of glaze underlying and the variability of the thickness of the enamel. The thickness of the overglaze decoration of the Qing Dynasty artifact can be very thin (up to $100\text{ }\mu\text{m}$ or a little less) [13,21]. On the contrary, the glazes of Yuan and Ming Dynasty blue-and-white porcelains are thicker ($200\text{--}500\text{ }\mu\text{m}$), and when the blue decoration is drawn on the body before the deposition of the glaze and firing, the diffusion of cobalt throughout the glaze thickness can be limited to the body–glaze interface layer [21,26,27]. The enamel matrix composition, in which the pigment bringing the blue color is dissolved, also varies. In addition, depending on the desired decoration, the concentration of the coloring agent will be different. Consequently, we compare the data with previous measurements [11,23,27,47,48], and some data is normalized with respect to the cobalt signal. The data clustering method serves to characterize the productions using identical or similar raw materials but also similar enamel thicknesses. Different clusters may be due to the use of different raw materials but also differences in the geometry of the enamel layers.

4.1. Glaze

We first compare the main elements associated with cobalt already present in the colorless glaze. As shown in Figures 3, 4 and 6 the colorless glaze is relatively rich in iron, manganese and also contains nickel and arsenic traces. It is almost free of cobalt traces. We therefore compare the relative intensities of the signals of these elements. All the objects present identical distributions for the precision of measurements concerning iron. Moreover, very comparable manganese and some variable nickel content are observed. Only the plate assigned to Meissen, Saxony (AR 2001-225) is differentiated regarding a higher arsenic trace content. As a first conclusion, all the colorless glazes of Chinese artifacts (whatever the type) have been made with similar raw materials, which supports their production

in Jingdezhen kilns. We can therefore compare the results for the areas colored in blue (overglaze). The errors induced by the silicate matrix constituting almost all of the enamel hardly disturb the elements studied. The data in the triple scattering plots (Figures 6–9) were normalized as explained in the experimental part. In brief, the sole elements shown in the figures were normalized via Rh counts, and for the comparison of the blue color, the data is normalized by cobalt and for the fluxes, normalized by Si, representing the major element of the matrix.

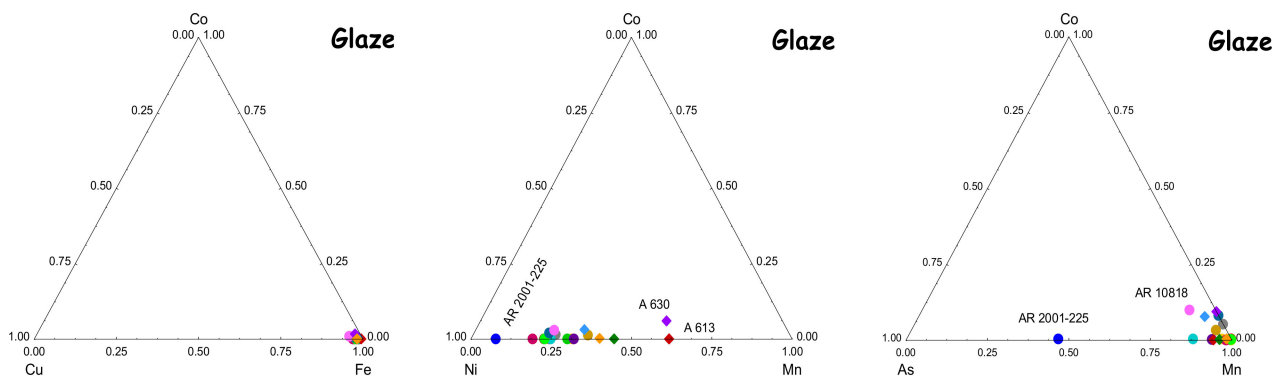


Figure 6. Comparison of the net number of XRF photons of the elements Co, Cu, Fe, Ni, Mn and As measured on the noncolored glaze. The objects listed in the Ariana Table (AR ### code) are shown with the colored solid circles and those of the Baur Table (A ### code) with the lozenges. The inventory numbers of objects located outside or on the edge of a cluster are indicated. Different colors of labels are used for didactic reasons.

4.2. Blue Areas

Regarding the objects in the Baur Collection (Table 2), two objects, bowls A 630 (second quarter of the 19th century, Daoguang reign) and A 613 (attributed to Kangxi), are distinguished by a higher level of manganese. On the contrary, the AR 2001-225 (Meissen dish) is Mn-poor but rich in nickel. The AR 10818 artifact (armorial export porcelain) also seems to have been made with raw materials, having less manganese trace content. The very limited dispersion of the data measured for the other artifacts, assigned to have been enameled/glazed in/for the Custom District in Gangzhou, is very consistent with the similarity deduced from the visual criteria. This point is discussed further.

Figure 7 compares the net number of X-ray photons emitted for the cobalt element with those of potassium and lead, characteristic elements of the two types of coating, a K-(Na cannot be observed) and Ca-based glaze fired at a higher temperature with the body (likely >1250–1300 °C), or a Pb-rich enamel fired at a lower temperature (~700–850 °C). In the latter case, the final firing(s) can be made in a place different from where the porcelain body is prepared and fired. It is commonly assumed that the porcelain bodies were prepared (and glazed) in Jingdezhen (imperial or private kilns) and the enameling to have also been made in Jingdezhen, Guangzhou or at the Forbidden city (Beijing) workshops. Figure 8 compares the cobalt content, always via the net number of X-ray photons emitted for the cobalt element with the similar signal of elements commonly associated with, i.e., arsenic, copper, nickel, manganese and iron, the relative content depending on the cobalt ores and the processing [23].

It appears that most of the blue areas analyzed on the objects, which were attributed to Jingdezhen, Guangzhou and Forbidden City workshops, present very comparable XRF signatures regarding the flux type of the blue-colored areas. The A 615 marks is a typical underglaze mark covered with a K-rich, lead-free or lead-poor glaze. Similar characteristics are measured for the A 613 mark, but visual examination is not clear. This supports the deposition of the two later marks on the body before the firing of the body and glaze at Jingdezhen (underglaze mark) for these two artifacts.

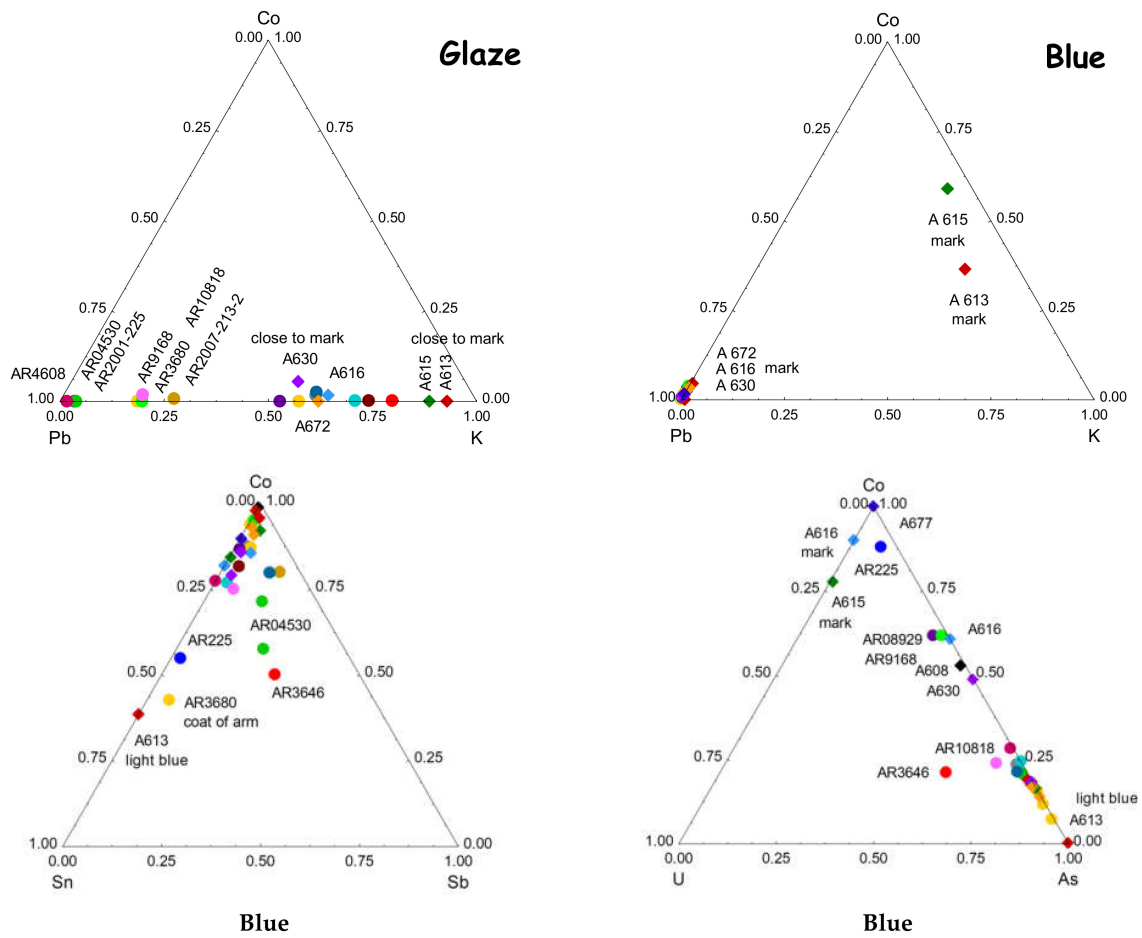


Figure 7. Comparison of the net number of XRF photons of the elements Co, Pb and K measured on the glaze and blue areas. Objects with special characteristics are labeled (see Tables 1 and 2). Sn, Sb, U and As content are also presented (left and right, bottom) for the blue-colored areas.

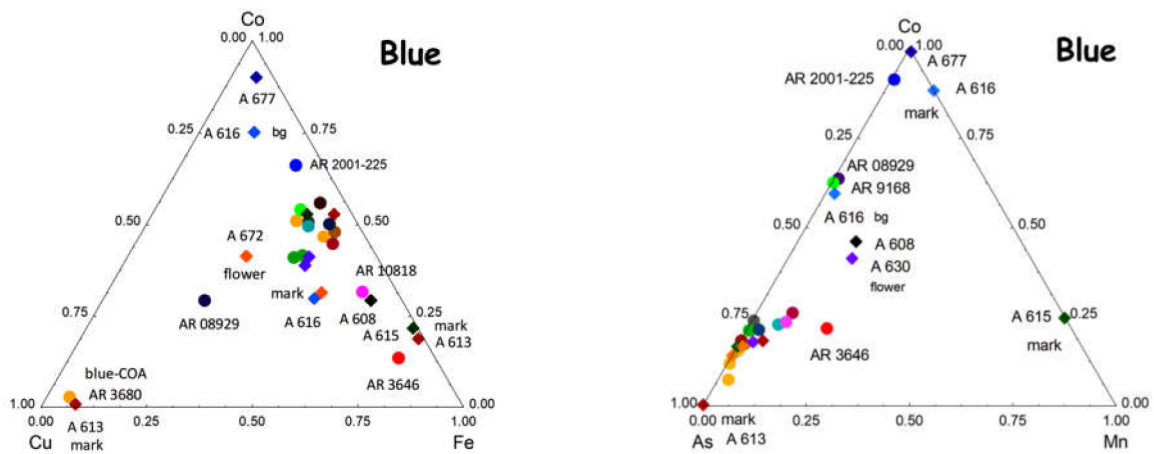


Figure 8. Cont.

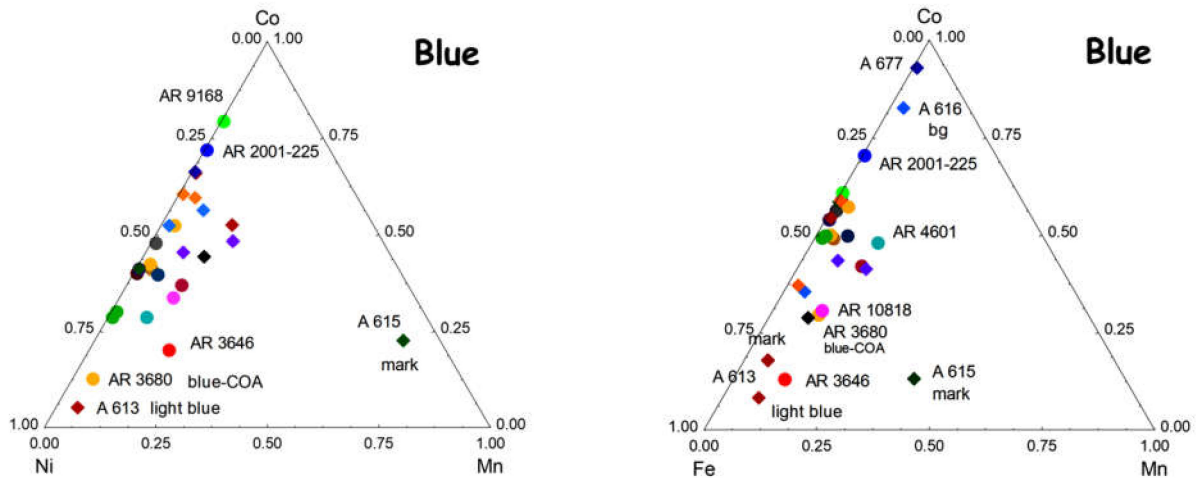


Figure 8. Comparison of the net number of XRF photons of the elements Co, Cu, Fe, Ni, Mn, and As measured on the blue areas and near the marks for the objects of the Ariana Table (circles; i.e., mostly assigned to Guangzhou customs) and the Baur Table (lozenges, assigned to the Imperial Beijing workshop). Objects with special characteristics are indicated (see Tables 1 and 2).

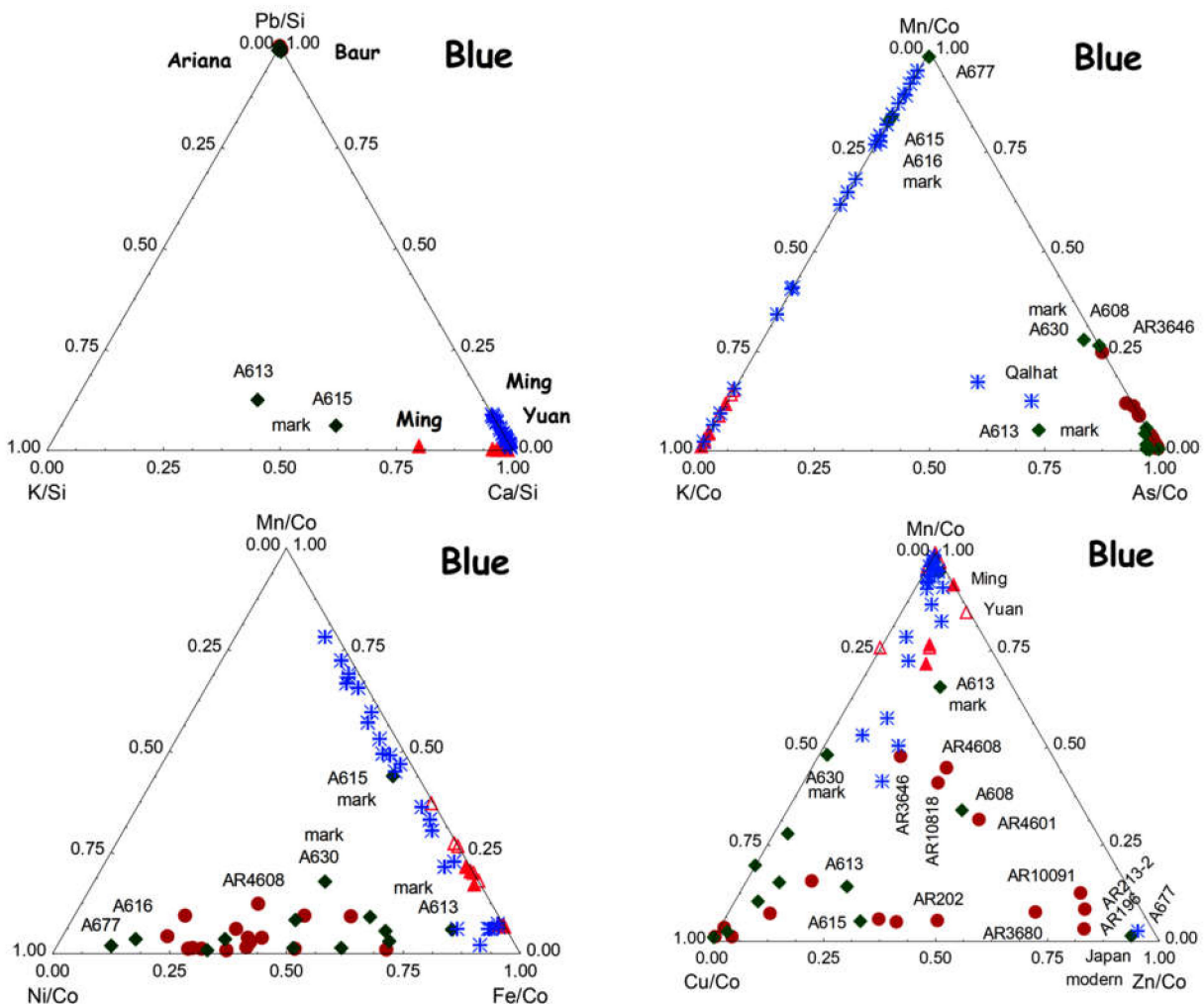


Figure 9. Cont.

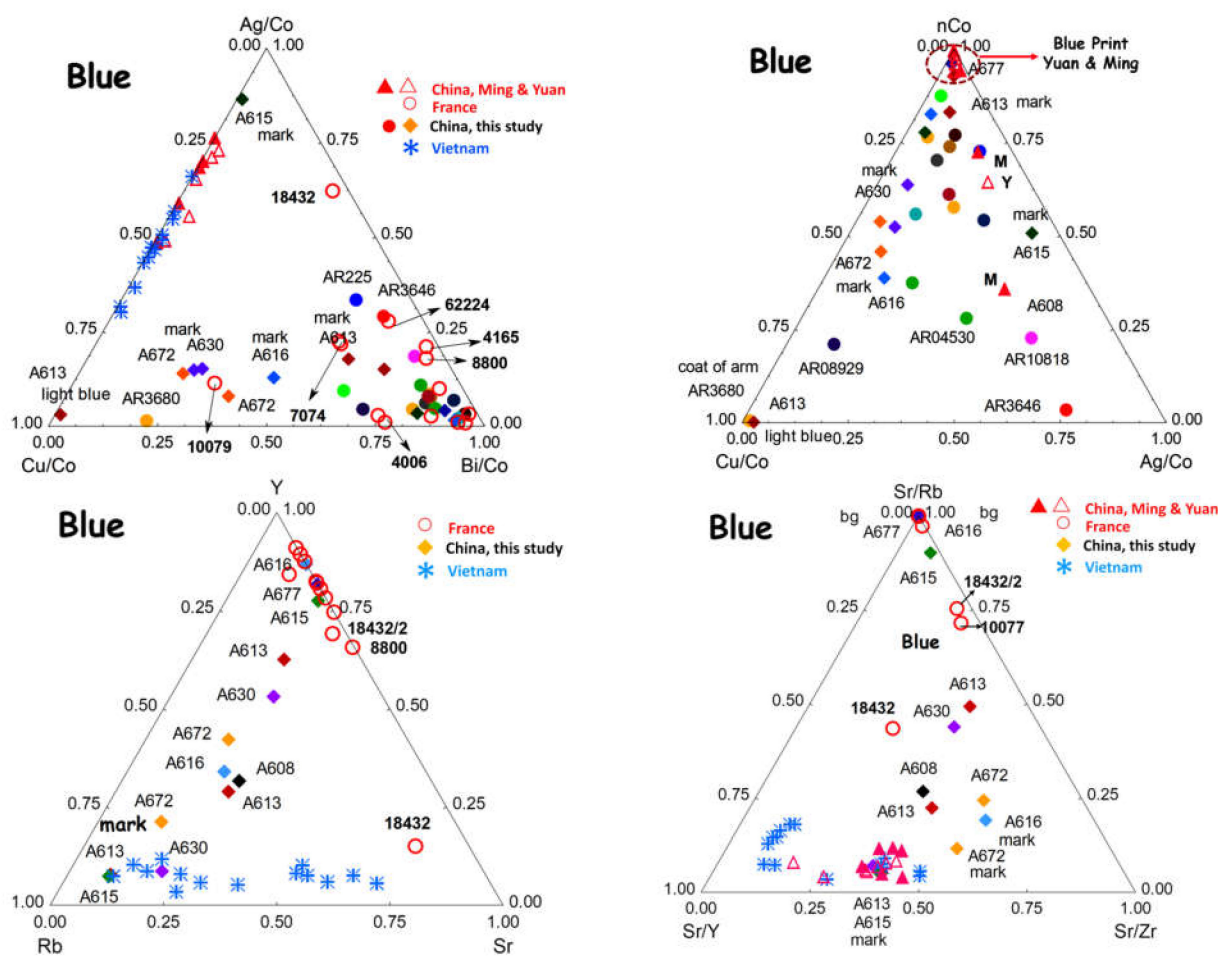


Figure 9. Comparison of the XRF signal for different elements of the blue enamel matrix (Pb, K, Ca, Fe, Ni, Rb, Sr, Y and Zr) and associated to cobalt blue (Mn, As, Cu, Zn, Bi and Ag) for artifacts of the present study (Tables 1 and 2) with a series of Chinese and Vietnamese blue-and-white porcelains from Yuan and Ming Dynasty periods [27,47,48]. Open (Yuan Dynasty) and closed (Ming Dynasty) red triangles are added from the data used in refs [46–48]. Blue stars correspond to the data used in ref. [27] relative to Vietnamese (Chù Dau, Vietnam and Qalhat, Oman Sultanate sites) and Chinese (China and Hoa Lu, Vietnam sites) porcelain/stoneware. Lozenges correspond to Table 1 (mostly Guangzhou workshops) and circles to Table 2 (Beijing Forbidden City workshop). Open red circles correspond to the blue-and-white decoration of French soft-paste porcelains from the 17th and early 18th centuries [50] and décor of enameled watches [11].

Three groups of glaze composition are identified, namely, lead-rich (AR 04530, AR 20001-225 (Meissen)), mixed lead–alkali/earth–alkali glaze (AR 9168 (19th century), AR 3680, AR 10818 and AR 2007-213-2) and lead-poor glaze (others). In the first two groups, we have only artifacts assigned to Guangzhou from the dates of production assigned mainly to the Qianlong period.

Examination of Sn, Sb, As and U signals in the blue areas shows the presence of different groups. For the blue mark of A 615, we have the maximum amount of U, and for A 616, AR 3646, AR 10818 and AR 225 the amount of U is significant. Erzgebirge where cobalt sources exist, has the ores of uranium associated with bismuth [49]. Many artifacts of the lead-rich glaze group also show a significant Sn and Sb content. On the other hand, the A 677, AR 225 (Meissen), A 616 and A 615 marks are arsenic-free, and another group is arsenic-poor (AR 08929 (Japan), AR 9168 (19th century), A 608 (dish) and A 630 (19th century)). The number of outliers being very limited, the blue coloring agent

used for artifacts assigned to Guangzhou workshops is obviously identical and rich in arsenic, as expected for cobalt-based ingredients imported from Europe [21,23].

We now examine the areas colored in blue in more detail (Figure 8):

- Arita porcelain (AR 8929, Japan): The blue is almost free of Mn, low in As and Ag but with Cu and a remarkably large amount of Bi. The observation of a high level of copper is consistent with the very early date of production (before 1700); the presence of bismuth is also consistent with a 17th century European cobalt. Indeed, similar things have been observed for very rare French soft-paste porcelain of the same period [50]. Similar features are observed for the A 613 mark and the coat-of-arms of the armorial porcelain dish (AR 3680), but not for the other blue areas of this dish; this indicates that copper was added to adjust the hue. On the contrary, as for Arita porcelain, the Cu-rich A 613 mark is consistent with a production of this bowl with a Kangxi mark with the ingredients first imported by Jesuits around 1690. Bowl A 613 is potentially also due to the characteristics of its gold decoration, one of the first pieces made under Kangxi with European recipes.
- The plate (AR 2001-225) is assigned to the Meissen factory (Saxony): The cobalt is quite pure, free of manganese and almost free of As, Ni and Fe, as are the A 677 decoration and the A 616 mark. Such a level of purity is strange, and the assignment of artifacts must be questioned. More artifacts assigned to the Meissen factory should be analyzed to draw a reasonable conclusion from these data.
- Bowls A 677 (attributed with reserves to the reign of Kangxi) and A 616 (attributed to the reign of Yongzheng, also with reserves) show the use of rather pure cobalt for the background: a smaller Fe and Cu and no Mn content. Assignment of the A 677 decoration made after 1850 is thus reasonable. The mark of the A 616 bowl uses a rather pure cobalt, but some other characteristics come close to those ascertained in the main group. The question now arises: is that consistent with the addition of the overglazed mark perhaps made on the bowl many years after its production?
- The 19th century box (AR 9168) is distinguished by its lower Mn content. A higher purification processing of cobalt ores was made after 1850 [23]. This is consistent with the stylistic assignment.
- The A 615 bowl mark is rich in Mn, as observed for artifacts produced during the Ming Dynasty [23,26,27,29,70–84,94–101]. A ‘return’ to traditional Chinese techniques has already been observed for Yongzheng productions [25].
- Objects A 608, A 630, AR 3646, AR 4601, AR 10818, AR 3680 and AR 3646 have a similar and higher Mn/Fe ratio (Figure 8) and are attributed to the Qianlong period; this higher Mn level is consistent with the use of a mixture of European and Asian cobalt to reduce the cost of production. The mixing of different sources, either to optimize the hue or reduce the cost was already reported [23]; we also observe a lower As content, as expected for such a mixture.

The comparison of the net number of XRF photons coming from Pb for the colorless glazes and blue-colored areas clearly shows that with the exception of the marks of bowls A 615 and A 613 produced with the underglaze technique (drawing directly over the clay before firing), all blue-colored areas are made of lead enamels. The different glaze compositions are clearly visible, namely, very potassic for A 630 and A 613, very rich in lead for AR 4530 and the Meissen plate (AR 2001-225), with the addition of lead for AR 9168 (Guangzhou, 19th century), AR 3680 (armorial porcelain) and AR 2007-213-2 (attributed to Jingdezhen).

4.3. Comparison with Previous (Yuan and Ming) Productions

The comparison using the same ternary diagrams with previous campaigns of XRF measurements, namely upon Vietnamese and Chinese porcelains from Yuan and Ming Dynasty periods [23,26,27,29,77–84,94–101] will help further the classification of the artifacts (Figure 9).

The use of lead-free glaze for the analyzed Yuan and Ming ceramics is obvious. The more interesting information is that all their (underglaze) blue decoration is free of arsenic as previously evidenced by many authors [11,23,47,48,50]. If a certain distribution inherent in the use of ores subjected to a visual selection but not having been the subject of a chemical refining is observed, it is limited and anisotropic depending on the geological context as previously reported [23]. The distributions concerning the studied artifacts are more important, in particular for the elements which depend on the process of refining.

The refining process, which was introduced in a significant way in the 18th century (involving the removal of the iron by acid attack, etc.), became more sophisticated in the 19th century [23]. Mn/Co-Ni/Co-Fe/Co, Mn/Co-Cu/Co-Zn/Co, Mn/Co-K/Co-As/Co and Ag/Co-Cu/Co-nCo (normalized by the X-ray tube, Rh count) diagrams perfectly separate the Qing Dynasty blues from the Ming and Yuan Dynasty ones. Only the cobalt of the A 615 mark is similar to the Ming blue. At the same time, the A 615 blue decoration belongs to the Qing group. Arsenic is definitively a signature of enameled artifacts made during the 18th century. Yuan and Ming blue areas are also free of nickel, copper, bismuth, silver and zinc. The latter elements are associated with the European cobalt ores [23,73–76]. The ratio of cobalt versus these elements is variable, firstly due to the intrinsic variability of content in the rock (in that case an approximate linear distribution starting from the major element (or ratio according to the mineral composition)) is observed on the ternary diagram [23], and secondly, due to the different selection and processing of the ores. We recall that European cobalt first was isolated as a byproduct of silver production (up to ~ the 15–16th centuries), then of silver and bismuth production (after the 15th century), and special extraction of cobalt is assumed to start during the 17th century [23].

It is interesting to compare the dispersion of the data measured for the productions of the different Dynasties; very little dispersion for Yuan and Ming productions and a wider dispersion for Qing productions are evidenced. In the first case, we have standardized productions using the same or seminal raw materials, and on the other hand, the variability can be linked to the use of a different cobalt, either because of different origins and/or mixtures, or the evolution of the rapid refining processes in relation with a high number of independent, private workshops.

The comparison of the data concerning the characteristic impurities of fluxes (Rb, Sr) or refractory raw materials (kaolin/pegmatites, etc., Y, Zr) confirms that the overglazes are profoundly different and that if the distribution of the data (limited here to objects in Table 2 for didactic reasons) is roughly aligned on a constant level of rubidium, they are very dispersed in Y and in Sr. This indicates that while some raw materials are common to all objects, others are not, testifying to the unique character of each enamel decoration.

Figure 10 compares hierarchical dendrograms of the blue-colored areas. The choice of data is like the other subjective visualization of the results. We selected the variables firstly to distinguish the main characteristics, namely K and Pb, representative of the two types of silicate matrix, glaze and overglaze, and then Mn and As, characteristic signals of the two types of cobalt ores. We observe the differentiation between the bowls of the Baur Foundation, supposedly enameled in the workshop of the Palace in Beijing, and the other objects supposedly made in workshops in Guangzhou. A third group of objects (n.r. labeled objects appearing on the right side of the dendrogram, Figure 10) is also evidenced: they contain pale-colored decorations, where their enamels appear very thin. We believe that the comparison is disturbed by the weakness of the signal of the elements associated with cobalt and the dominant contribution of the underlayer glaze. The bowl A 677 presents many contradictory characteristics with its mark, and therefore its dating must be considered quite apart.

The ternary diagrams of Figure 9 show the signals Mn, Ni and Fe as well as Ag, Cu and Bi normalized to cobalt to classify objects of any origin (the Yuan and Ming Dynasty periods, the Qing Dynasty). The comparison of the signals of these elements should make it possible to classify the enamels with respect to the sources of cobalt (ores and processing/refining of cobalt). It is important to note that the data measured on the blue-colored areas of

blue-and-white soft-paste French porcelains from the 17th and early 18th centuries [50] and enamelled watches from the same period [10] are located in the same cluster as Imperial and Gangzhou wares in the Ag–Cu–Bi (normalized by Co) ternary diagram (Figure 9). This definitively confirms the use of imported cobalt. The observation of the ternary Y–Rb–Sr, characteristic impurities of the raw materials used to produce the silicate matrix of the enamel, shows that the enameled objects in France form a very different cluster from the enameled objects in Guangzhou or Beijing, except the A615, A616 and A 677. Therefore, for the other objects only the coloring matter was imported from Europe, while it is probable that for the three objects belonging to the same cluster the complete enamel powder was imported. Bowls A 613 and A 677 bear the marks of the reign of Kangxi and A 616 of Yongzheng.

The hierarchical classification is used in Figure 10. The classification works quite well by considering the signals of Mn, As, Ni and Fe characteristic of cobalt. Only the object AR 3680 (Armorial decoration) is in the group of ‘Imperial’ objects. On the other hand, the blue areas of A 630 (Daoguang), A 608 (Qianlong dish), A 616 (uncertain Yongzheng) and A 677 (uncertain Kangxi) are in the same group as the enamels attributed to the Guangzhou workshops. These last two artifacts being at the end of the dendrogram, the questionable character of their dating from the marks is therefore reinforced.

The use of a maximum number of signals is deemed to be more relevant, but in the case of the observation on an intrinsically nonhomogeneous material and with respect to the depth analyzed according to the element considered, the result is also more sensitive to pollution by the support. The separation is effective, except for the A 672 (Kangxi bowl), A 608 (Qianlong dish) and the mark of A 616 (Yongzheng questionable). The A 677 (uncertain Kangxi) is found well in the group of imperial bowls but isolated at the end.

The hierarchical classification does not explicitly give a positive or negative answer. The attribution depends on the variables and their reliability, which can vary from one artifact to another by considering the intensity of the color, the thickness of the enamel layer, etc. The introduction of parameters characteristic of the enamel composition reinforces the identification of the differences associated with those of the coloring matters.

The dendrogram in Figure 10 from the normalized Mn–Ni–Fe signals compares the data obtained on objects from the Qing Dynasty (shown with the red line for Imperial and blue line for Guangzhou objects) with those from the Yuan and Ming Dynasties, produced in China or Vietnam (shown in black lines). These data were also plotted in the scattering ternary diagrams (Figure 9), including the previously published objects [27,46–48] (shown with open brown circles and blue stars). The classification is almost perfect: the outliers, namely the character of the A 613 blue mark and the flower confirms that ‘ancient’ Ming recipes/raw materials were used for these colored areas. It is also consistent that the 19th century artefact introduced as comparison in the Qing Dynasty series exhibits a different signature. The other dendrograms, which include the correlation of the objects via the major, minor and trace elements found in the blue-colored areas in Figure 10, also allows to distinguish the Imperial and Guangzhou productions. The error factor is higher for the thinner objects (shown with n.r. (not reliable) code), thus grouping them separately from the other objects.

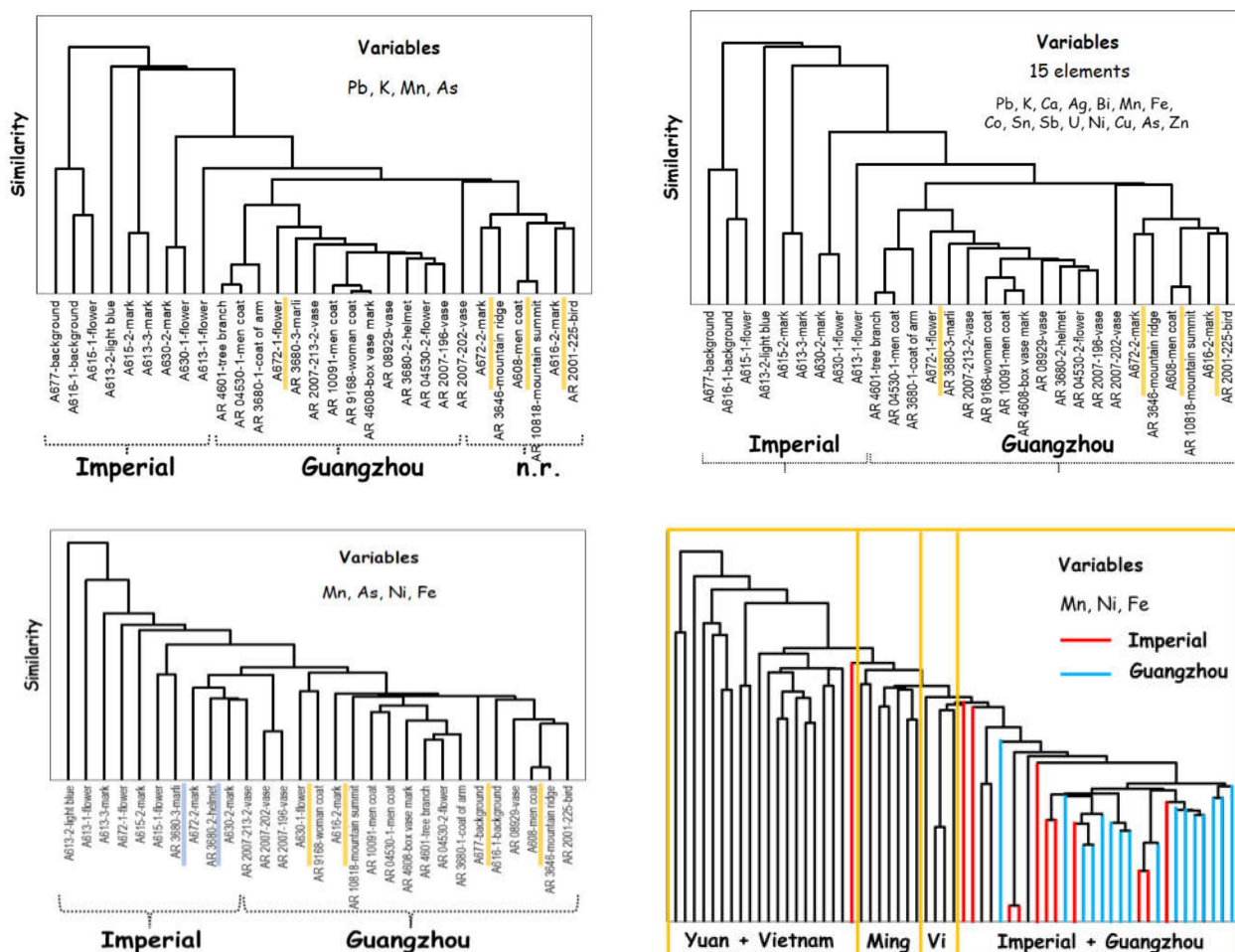


Figure 10. Hierarchical Euclidian diagrams which were drawn from the calculation of different variables referring to Tables 1 and 2 artifacts; net number of X-ray photons of Pb, K, Mn and As (top, left); Mn, As, Ni and Fe (bottom, left); 15 elements recorded for the blue area (top, right) and Mn, Ni and Fe referring to the studied artifacts (attributed to “Imperial” and “Guangzhou”) in comparison with a series of Chinese and Vietnamese blue-and-white porcelains from the Yuan and Ming Dynasty periods (unlabeled; from the left to the right hand, isolated artifacts are A 615 Yongzheng mark, A 613 Kangxi mark and A 613 flower; the isolated Guangzhou is AR 9168 women’s coats (19th century; for comparison)) n.r.: nonreliable data; we explain this group arises from the very thinness of the enamels that makes an important contribution to the substrate and hence dominates the characteristics of these data. Yellow (Imperial) and blue (Guangzhou) underlines are used to draw the attention of the reader by highlighting the outliers of a group.

5. Conclusions

Comparison of the net number of XRF photons recorded with mobile instruments on-site, without defining the chemical composition semiquantitatively, allows the analysis of outstanding artifacts. The three-dimensional heterogeneity of the colored zones led us to compare the data in the number of photons by looking at the ratios of elements which appeared to us by reasoning to be relevant. In front of our view, this approach seems more reasonable than a simple multivariate approach (PCA). It would, however, be interesting to see what a supervised or more sophisticated multivariate approach would give (neural network). Their priceless values act against their displacement to the laboratory and also a fortiori sampling is prohibited. Comparison with significant series of previous data recorded with different instruments (Bruker Tracer and Elio pXRFs) leads to support the discussion after normalization of the data. The similarity of the glaze composition is

consistent with the assumption that all the porcelain bodies have been made and glazed at Jingdezhen or with raw materials identical to those used at Jingdezhen. Highly grouped data for the blue areas of objects attributed to Guangzhou from the Kangxi and Yongzheng periods indicate the use of the same raw materials imported from Europe, which provides cobalt associated with some characteristic elements (chiefly As but also Bi, Zn and Ag). This corroborates the assumption of the Jesuit Father Dentrecolles, who stated that some enamels used in Jingdezhen came from Beijing and Guangzhou when he came to observe the Jingdezhen manufacturing process during the first decade of the 18th century [102]. The consistent shift in data was noted for the Qianlong style items, especially richer in manganese, which is consistent for mixing with Asian cobalt, probably in order to reduce the production costs. The situation is identical for the A 608 (Qianlong reign) and A 630 (Daoguang reign) objects. The objects chosen as counterexamples belonging to other places of production or other periods are well-observed outside of the clusters of the family studied. Some specificity is measured for artifacts assigned to the Forbidden City (Figure 10). The analysis highlights the objects with specific compositional criteria outside of the 'main' data cluster and having characteristics of anachronistic purity. Two objects with the Imperial mark, on which certain reservations concerning the assignment had been made with respect to the stylistic analysis, are clearly examples of ceramics containing a refined 'cobalt' and can therefore be assigned to a production date later than the first half of the 19th century. For a small number of artifacts, it seems that the compromising of the measurement by the materials under the enamel layer makes difficult the comparison of the data: this takes place for the AR 3646, A 608, AR 10818, AR 20001-225 and one of the measurements of the A 616 mark; a visual examination points out that the blue layer is actually very thin for these examples.

If the collection of the elemental data on-site in a noninvasive way and advanced treatment of the data allowing the classification of the artifacts and identification of outliers is generally possible, it is not possible to obtain a clear-cut answer in all cases. Experimental arguments support the reservation expressed by some scholars on two imperial bowls. The question relative to the artifact assigned to Meissen motivates further specific analyses of a different series of artifacts assumed to be produced in Meissen and its use of the application of colored decoration many years after the production of the porcelain body in question.

Author Contributions: Conceptualization, P.C. and P.d.; methodology, P.C., M.G. and G.S.F.; investigation, P.C. and M.G.; writing—original draft preparation, P.C., G.S.F. and P.d.; writing—review and editing, P.C., G.S.F., M.G., P.d. and A.-C.S. All authors have read and agreed to the published version of the manuscript.

Funding: This research received no external funding.

Institutional Review Board Statement: Not applicable.

Data Availability Statement: Not applicable.

Acknowledgments: Laure Schwartz Arenales (Director of Fondation Baur, Musée des arts d'Extrême-Orient) and Isabelle Naef Galuba (Director of Ariana Museum) are cordially thanked for their support and their authorization to study the artefacts.

Conflicts of Interest: The authors declare no conflict of interest.

References

1. Curtis, E.B. European Contributions to the Chinese Glass of the Early Qing Period. *J. Glass. Stud.* **1993**, *35*, 91–101.
2. Shih, C.F. Evidence of East-West exchange in the eighteenth century: The establishment of painted enamel art at the Qing Court in the reign of Emperor Kangxi. *Natl. Palace Mus. Res. Q.* **2007**, *24*, 45–94.
3. Zhou, S.Z. *Research on Painted Enamels Porcelain Ware from the Qing Court*; Wenwu Chubanshe: Beijing, China, 2008.
4. Curtis, E.B. *Glass Exchange between Europe and China, 1550–1800*; Ashgate: Farnham, UK, 2009.
5. Lili, F. *La Céramique Chinoise*; China Intercontinental Press: Beijing, China, 2011.
6. Shih, C.F. *Radiant Luminance: The Painted Enamelware of the Qing Imperial Court*; The National Palace Museum of Taipei: Taipei, Taiwan, 2012.

7. Xu, X.D. Europe-China-Europe: The Transmission of the Craft of Painted Enamel in the Seventeenth and Eighteenth Centuries. In *Goods from the East, 1600–1800 Trading Eurasia*; Berg, M., Ed.; Palgrave Macmillan: London, UK, 2015; pp. 92–106.
8. Zhao, B.; Wang, G.Y.; Biron, I.; Colomban, P.; Hilaire-Pérez, L. La Circulation des Techniques de l'émail Entre la France et la Chine du XVIIème au XIXème Siècle. *CNRS Chine Bull.* **2016**, *21*, 20–25. Available online: http://www.cnrs.fr/derci/IMG/pdf/cnrsechine_21_fr_final_pour_le_site_cnrs.pdf (accessed on 15 December 2019).
9. Tang, H. The Colours of Each Piece: Production and Consumption of Chinese Enamelled Porcelain, c.1728–c.1780. Ph.D. Thesis, University of Warwick, Warwick, UK, 2017. Available online: <http://webcat.warwick.ac.uk/record=b3099976~|S15> (accessed on 30 May 2022).
10. Colomban, P.; Arberet, L.; Kırmızı, B. On-Site Raman Analysis of 17th and 18th Century Limoges Enamels: Implications on the European Cobalt Sources and the Technological Relationship between Limoges and Chinese Enamels. *Ceram. Int.* **2017**, *43*, 10158–10165. [[CrossRef](#)]
11. Colomban, P.; Kırmızı, B.; Gougeon, C.; Gironde, M.; Cardinal, C. Pigments and glassy matrix of the 17th–18th century enamelled French watches: A non-invasive on-site Raman and pXRF study. *J. Cult. Herit.* **2020**, *44*, 1–14. [[CrossRef](#)]
12. Colomban, P.; Zhang, Y.; Zhao, B. Non-invasive Raman analyses of *huafalang* and related porcelain wares. Searching for evidence for innovative pigment technologies. *Ceram. Int.* **2017**, *43*, 12079–12088. [[CrossRef](#)]
13. Colomban, P.; Ambrosi, F.; Ngo, A.-T.; Lu, T.-A.; Feng, X.-L.; Chen, S.; Choi, C.-L. Comparative analysis of *wucui* Chinese porcelains using mobile and fixed Raman microspectrometers. *Ceram. Int.* **2017**, *43*, 14244–14256. [[CrossRef](#)]
14. Ma, H.J.; Henderson, J.; Cui, J.F.; Chen, K.L. Glassmaking of the Qing Dynasty: A review, New Data and New Insights. *Adv. Archaeom.* **2020**, *1*, 27–35. [[CrossRef](#)]
15. Howard, D. *Chinese Armorial Porcelain*; Faber & Faber: London, UK, 1952; Volume 1.
16. Jourdain, M.; Soame, J. *Chinese Export Art in the 18th Century*; Spring Books: Feltham, UK, 1967.
17. Le Corbeiller, C. China trade armorial porcelain in America. *Antiques* **1977**, *12*, 1124–1129.
18. Godden, G.A. *Oriental Export Market Porcelain and Its Influence on European Wares*; Grenada: London, UK, 1979.
19. Howard, D.S. *Chinese Armorial Porcelain*; Heirloom & Howard: London, UK, 2003; Volume 2.
20. Lebel, A. *Armoiries Françaises et Suisses sur la Porcelaine de Chine au XVIIIe Siècle*; Antoine Lebel: Bruxelles, Belgium, 2009.
21. Colomban, P.; Ngo, A.-T.; Fournery, N. Non-invasive Raman Analysis of 18th Century Chinese Export/Armoirial Overglazed Porcelain: Identification of the Different Enameling Technology. *Heritage* **2022**, *5*, 233–259. [[CrossRef](#)]
22. Watt, J.C.Y. Notes on the Use of Cobalt in Later Chinese Ceramics. *Ars Orient.* **1979**, *11*, 63–85.
23. Colomban, P.; Simsek Franci, G.; Kırmızı, B. Cobalt and Associated Impurities in Blue (and Green) Glass, Glaze and Enamel: Relationships between Raw Materials, Processing, Composition, Phases and International Trade. *Minerals* **2021**, *11*, 633. [[CrossRef](#)]
24. Colomban, P.; Kırmızı, B.; Zhao, B.; Clais, J.-B.; Yang, Y.; Droguet, V. Non-invasive on-site Raman study of pigments and glassy matrix of the 17th–18th century painted enamelled Chinese metal wares: Comparison with French enamelling technology. *Coatings* **2020**, *10*, 471. [[CrossRef](#)]
25. Colomban, P.; Gironde, M.; Vangu, D.; Kırmızı, B.; Zhao, B.; Cochet, V. The technology transfer from Europe to China in the 17th–18th centuries: Non-invasive on-site XRF and Raman analyses of Chinese Qing Dynasty enameled masterpieces made using European ingredients/recipes. *Materials* **2021**, *14*, 7434. [[CrossRef](#)]
26. Colomban, P.; Sagon, G.; Huy, L.Q.; Liem, N.Q.; Mazerolles, L. Vietnamese (15th Century) lue-and-white tam thai and luster porcelains/stonewares: Glaze composition and decoration techniques. *Archaeometry* **2004**, *46*, 125–136. [[CrossRef](#)]
27. Simsek, G.; Colomban, P.; Wong, S.; Zhao, B.; Rougeulle, A.; Liem, N.Q. Toward a fast non-destructive identification of pottery: The sourcing of 14th–16th century Vietnamese and Chinese ceramic shards. *J. Cult. Herit.* **2015**, *16*, 159–172. [[CrossRef](#)]
28. Van Pevenage, J.; Lauwers, D.; Herremans, D.; Verhaeven, E.; Vekemans, B.; De Clercq, W.; Vincze, L.; Moens, L.; Vandnabeele, P. A Combined Spectroscopic Study on Chinese Porcelain Containing Ruan-Cai Colours. *Anal. Methods* **2014**, *6*, 387–394. [[CrossRef](#)]
29. Giannini, R.; Freestone, I.; Shortland, A.J. European cobalt sources identified in the production of Chinese *Famille rose* porcelain. *J. Archaeol. Sci.* **2017**, *80*, 27–36. [[CrossRef](#)]
30. Colomban, P.; Kırmızı, B. Non-invasive on-site Raman study of polychrome and white enamelled glass artefacts in imitation of porcelain assigned to Bernard Perrot and his followers. *J. Raman Spectrosc.* **2020**, *51*, 133–146. [[CrossRef](#)]
31. Colomban, P.; Lu, T.-A.; Milande, V. Non-invasive on-site Raman study of blue-decorated early soft-paste porcelain: The use of arsenic-rich (European) cobalt ores—Comparison with *huafalang* Chinese porcelains. *Ceram. Int.* **2018**, *44*, 9018–9026. [[CrossRef](#)]
32. Colomban, P.; Maggetti, M.; d'Albis, A. Non-invasive Raman identification of crystalline and glassy phases in a 1781 Sèvres Royal Factory soft paste porcelain plate. *J. Eur. Ceram. Soc.* **2018**, *38*, 5228–5233. [[CrossRef](#)]
33. Colomban, P.; Sagon, G.; Faurel, X. Differentiation of antique ceramics from the Raman spectra of their coloured glazes and paintings. *J. Raman Spectrosc.* **2001**, *32*, 351–360. [[CrossRef](#)]
34. Ricciardi, P.; Colomban, P.; Tournié, A.; Milande, V. Nondestructive on-site identification of ancient glasses: Genuine artefacts, embellished pieces or forgeries? *J. Raman Spectrosc.* **2009**, *40*, 604–617. [[CrossRef](#)]
35. Zhou, Y.; Jin, Y.; Wang, K.; Sun, J.; Cui, Y.; Hu, D. Opaque ancient K₂O-PbO-SiO₂ glass of the Southern Song Dynasty with fluorite dendrite and its fabrication. *Herit. Sci.* **2019**, *7*, 56. [[CrossRef](#)]
36. Colomban, P. Rocks as blue, green and black pigments/dyes of glazed pottery and enameled glass artefacts—A review. *Eur. J. Miner.* **2014**, *25*, 863–879. [[CrossRef](#)]

37. Sakellariou, K.; Miliiani, C.; Morresi, A.; Ombelli, M. Spectroscopic investigation of yellow majolica glazes. *J. Raman Spectrosc.* **2004**, *35*, 61–67. [[CrossRef](#)]
38. Sandalinas, C.; Ruiz-Moreno, S.; Lopez-Gil, A.; Miralles, J. Experimental confirmation by Raman spectroscopy of a Pb-Sn-Sb triple oxide yellow pigment in sixteenth-century Italian pottery. *J. Raman Spectrosc.* **2006**, *37*, 1146–1153. [[CrossRef](#)]
39. Rosi, F.; Manuali, V.; Miliiani, C.; Brunetti, B.G.; Sgamellotti, A.; Grygar, T.; Hradil, D. Raman scattering features of lead pyroantimonate compounds. Part I: XRD and Raman characterization of Pb₂Sb₂O₇ doped with tin and zinc. *J. Raman Spectrosc.* **2009**, *40*, 107–111. [[CrossRef](#)]
40. Pereira, M.; de Lacerda-Aroso, T.; Gomes, M.J.M.; Mata, A.; Alves, L.C.; Colombar, P. Ancient Portuguese ceramic wall tiles (“Azulejos”): Characterization of the glaze and ceramic pigments. *J. Nano Res.* **2009**, *8*, 79–88. [[CrossRef](#)]
41. Pelosi, C.; Agresti, G.; Santamaria, U.; Mattei, E. Artificial yellow pigments: Production and characterization through spectroscopic methods of analysis. *e-Preserv. Sci.* **2010**, *7*, 108–115.
42. Rosi, F.; Manuali, V.; Grygar, T.; Bezdzicka, P.; Brunetti, B.G.; Sgamellotti, A.; Burgio, L.; Seccaroni, C.; Miliiani, C. Raman scattering features of lead pyroantimonate compounds: Implication for the non-invasive identification of yellow pigments on ancient ceramics. Part II. In situ characterisation of Renaissance plates by portable micro-Raman and XRF studies. *J. Raman Spectrosc.* **2011**, *42*, 407–414. [[CrossRef](#)]
43. Cartechini, L.; Rosi, F.; Miliiani, C.; d’Acapito, F.; Brunetti, G.; Sgamellotti, A.A. Modified Naples yellow in Renaissance majolica: Study of Pb-Sb-Zn and Pb-Sb-Fe ternary pyroantimonates by X-ray absorption spectroscopy. *J. Anal. At. Spectrom.* **2011**, *26*, 2500–2507. [[CrossRef](#)]
44. Colombar, P. The Use of Metal Nanoparticles to Produce Yellow, Red and Iridescent Colour, from Bronze Age to Present Times in Lustre Pottery and Glass: Solid State Chemistry, Spectroscopy and Nanostructure. *J. Nano Res.* **2009**, *8*, 109–132. [[CrossRef](#)]
45. Geyssant, J. Secret du verre rouge transparent de Bernard Perrot et comparaison avec celui de Johann Kunckel. In *Bernard Perrot (1640–1709), Secrets et Chefs-d’œuvre des Verreries Royales d’Orléans, Catalogue*; Klinka Ballesteros, I., de Valence, C., Maitte, C., Ricke, H., Eds.; Musée des Beaux-Arts d’Orléans—SOMOGY Editions d’Arts: Paris, France, 2013; pp. 51–54.
46. Colombar, P.; Liem, N.Q.; Sagon, G.; Tinh, H.X.; Hoành, T. Microstructure, composition and processing of 15th century Vietnamese porcelains and celadons. *J. Cult. Herit.* **2003**, *4*, 187–197. [[CrossRef](#)]
47. Simsek Franci, G. Blue Print: Archaeometric Studies of Colored Glazed Chinese Ceramics and Production of Replica, Final Report, The Scientific and Research Council of Turkey, The Scientific and Technological Projects Funding Program. *Unpublished Report*, 3 January 2021.
48. Simsek Franci, G. Handheld X-ray Fluorescence (XRF) versus wavelength dispersive XRF: Characterization of Chinese blue and white porcelain sherds using handheld and laboratory-type XRF instruments. *Appl. Spectrosc.* **2020**, *74*, 314–322. [[CrossRef](#)]
49. Kissin, S.A. Five-element (Ni-Co-As-Ag-Bi) veins. *Geosci. Can.* **1992**, *19*, 113–124.
50. Colombar, P.; Girona, M.; Edwards, H.G.M.; Mesqui, V. The enamels of the first (softpaste) European blue-and-white porcelains: Rouen, Saint-Cloud and Paris factories: Complementarity of Raman and X-ray fluorescence analyses with mobile instruments to identify the cobalt ore. *J. Raman Spectrosc.* **2021**, *52*, 2246–2261. [[CrossRef](#)]
51. Available online: <https://xrfcheck.bruker.com/InfoDepth> (accessed on 2 June 2022).
52. Ayers, J. *The Baur Collection, Geneva-Chinese Ceramics, Volume IV: Painted and Polychrome Porcelains of the Ch’ing Dynasty*; Collection Baur: Genève, Switzerland, 1974.
53. Garner, H. The Origins of Famille Rose. *Trans. Orient. Ceram. Soc.* **1967–1969**, *37*, 1–16. Available online: <https://www.orientalceramicsociety.org.uk/publications/transactions/4> (accessed on 2 June 2022).
54. Loehr, G. Missionary-artists at the Manchu Court. *Trans. Orient. Ceram. Soc.* **1962–1963**, *34*, 51–67. Available online: <https://www.orientalceramicsociety.org.uk/publications/transactions/4> (accessed on 2 June 2022).
55. Ayers, J. *Chinese Ceramics in the Baur Collection*; Collection Baur: Genève, Switzerland, 1999; Volume 2.
56. Shih, C.F. Cultural Contending: Kangxi Painted Enamelware as Global Competitor. *Minsu Quyi* **2013**, *182*, 149–219. (In Chinese)
57. Pierson, S. True or False? Defining the Fake in Chinese porcelain. *Cah. Fram.* **2019**, *31*, 6168. [[CrossRef](#)]
58. Qintero Pérez, A.; Anthonioz, S. *Chrysanthèmes, Dragons et Samourais. La Céramique Japonaise du Musée Ariana. L’Ariana Sort de Ses Réserves IV*; Catalogue, Georg Editeur: Geneva, Switzerland, 2020.
59. Guo, X.L. Guangcai qiyuan ji qi zaoqi mianmao [Origin and appearance of early Guangcai wares]. *Orient. Collect.* **2018**, *12*, 5–22.
60. Yang, G. A Pair of Canton Enamel Porcelain Masterpieces in the Rijksmuseum. *Aziat. Kunst* **2018**, *48*, 54–59. [[CrossRef](#)]
61. Schumacher, A.-C. (Ed.) *La Donation Clare van Beusekon-Hamburger: Faïence et Porcelaines des XVIe-XVIIIe Siècles*; Skira: Genève, Switzerland, 2010.
62. Available online: https://www.musee-ariana.ch/collections/search?f%5B0%5D=lieux_de_creation%3A1691&date_end=1780&date_start=1700&material=porcelaine&decor_and_iconography=famille%20rose&tab=vdg_artwork (accessed on 30 May 2022).
63. Impey, O. *The Early Porcelain Kilns of Japan*; Clarendon Press: Oxford, UK, 1996.
64. Nagatake, T. *Classic Japanese Porcelain—Imari and Kakiemon*; Kodansha International: Tokyo, Japan, 2003.
65. Murakami, N. *The Origin of Imari Porcelain—Excavated Shards from Komizo Kiln*; Sojusha Art Publishing: Tokyo, Japan, 2020. (In Japanese)
66. Montanari, R.; Murakami, N.; Alberghina, M.F.; Pelosi, C.; Schiavone, S. The Origin of overglaze-blue enameling in Japan: New discoveries and a reassessment. *J. Cult. Herit.* **2019**, *37*, 94–102. [[CrossRef](#)]
67. Fitski, M. *Kakiemon Porcelain—Handbook*; Leiden University Press: Leiden, The Netherlands, 2011.

68. Kysuhu Ceramic Museum (Ed.) *Kakiemon—The Whole Aspect of the Kakiemon Style—Special Exhibition Catalog*; Kysuhu Ceramic Museum: Kysuhu, Japan, 1999. (In Japanese)
69. Montanari, R.; Murakami, N.; de Bonis, A.; Colomban, P.; Alerghina, M.F.; Grifa, C.; Izzo, F.; Morra, V.; Pelosi, C.; Schiavone, S. The early porcelain kilns of Arita: Identification of raw materials and their use from the 17th to the 19th century. *Open Ceram.* **2022**, *9*, 100217. [[CrossRef](#)]
70. Manoun, B.; Azdouz, M.; Azrou, M.; Essehli, R.; Benmokhtar, S.; El Ammari, L.; Ezzahi, A.; Ider, A.; Lazor, P. Synthesis, Rietveld refinements and Raman spectroscopic studies of tricationic lacunar apatites $\text{Na}_{1-x}\text{K}_x\text{Pb}_4(\text{AsO}_4)_3$ ($0 < x < 1$). *J. Mol. Struct.* **2011**, *986*, 1–9. [[CrossRef](#)]
71. Colomban, P.; Ngo, A.-T.; Edwards, H.G.M.; Prinsloo, L.C.; Esterhuizen, L.V. Raman identification of the different glazing technologies of Blue-and-White Ming porcelains. *Ceram. Int.* **2021**, *48*, 1673–1681. [[CrossRef](#)]
72. Colomban, P. Full Spectral Range Raman Signatures Related to Changes in Enameling Technologies from the 18th to the 20th Century: Guidelines, Effectiveness and Limitations of the Raman Analysis of the Raman Analysis. *Materials* **2022**, *15*, 3158. [[CrossRef](#)]
73. Gratuze, B.; Soulier, I.; Barrandon, J.N.; Foy, D. De l'origine du cobalt dans les verres. *Rev. d'Archéom.* **1992**, *16*, 97–108. Available online: https://www.persee.fr/doc/arsci_0399-1237_1992_num_16_1_895 (accessed on 2 June 2022). [[CrossRef](#)]
74. Gratuze, B.; Soulier, I.; Blet, M.; Vallauri, L. De l'origine du cobalt: Du verre à la céramique. *Revue d'Archéom.* **1996**, *20*, 77–94. Available online: https://www.persee.fr/doc/arsci_0399-1237_1996_num_20_1_939 (accessed on 2 June 2022). [[CrossRef](#)]
75. Porter, Y. Le cobalt dans le monde Iranien (IXe-XVIe siècles). *Taoci* **2000**, *1*, 5–14.
76. Matin, M.; Pollard, A.M. From ore to pigment: A description of the minerals and experimental study of cobalt ore processing from the Kâshân mine, Iran. *Archaeometry* **2017**, *59*, 731–746. [[CrossRef](#)]
77. Wen, J.X.; Chen, Z.K.; Zeng, Q.G.; Hu, L.S.; Wang, B.; Shi, J.P.; Zhang, G.X. Multi-micro analytical studies of blue-and-white porcelain (Ming dynasty) excavated from Shuangchuan island. *Ceram. Int.* **2019**, *45*, 13362–13368. [[CrossRef](#)]
78. Jiang, X.; Ma, Y.; Chen, Y.; Li, Y.; Ma, Q.; Zhang, Z.; Wang, C.; Yang, Y. Raman analysis of cobalt blue pigment in blue and white porcelain: A reassessment. *Spectrochim. Acta Part A Mol. Biomol. Spectrosc.* **2018**, *190*, 61–67. [[CrossRef](#)] [[PubMed](#)]
79. Wang, T.; Zhu, T.Q.; Feng, Z.Y.; Fayard, B.; Pouyet, E.; Cotte, M.; De Nolf, W.; Sciau, P. Synchrotron radiation-based multi-analytical approach for studying underglaze color: The microstructure of Chinese Qinghua blue decors (Ming dynasty). *Anal. Chim. Acta* **2016**, *928*, 20–31. [[CrossRef](#)]
80. Wen, R.; Wang, C.S.; Mao, Z.W.; Huang, Y.Y.; Pollard, A.M. The chemical composition of blue pigment on Chinese blue-and-white porcelain of the Yuan and Ming Dynasties (AD 1271–1644). *Archaeometry* **2007**, *49*, 101–115. [[CrossRef](#)]
81. Zhou, Y.H.; Hu, Y.J.; Tao, Y.; Sun, J.; Cui, Y.; Wang, K.; Hu, D.B. Study on the microstructure of the multilayer glaze of the 16th–17th century export blue-and-white porcelain excavated from Nan'ao Shipwreck. *Ceram. Int.* **2016**, *42*, 17456–17465. [[CrossRef](#)]
82. Zhang, R.; Garachon, I.; Gethin, P.; van Campen, J. Double layers glaze analysis of the Fujian export blue-and-white porcelain from the Witte Leeuw shipwreck (1613). *Ceram. Int.* **2020**, *46*, 13474–13481. [[CrossRef](#)]
83. De Pauw, E.; Track, P.; Verhaeven, E.; Bauters, S.; Acke, L.; Vekemans, B.; Vincze, L. Microbeam X-ray fluorescence and X-ray absorption spectroscopic analysis of Chinese blue-and-white porcelain dating from the Ming dynasty. *Spectrochim. Acta Part B* **2018**, *149*, 190–196. [[CrossRef](#)]
84. Duan, H.; Zhang, X.; Kang, B.; Wang, G.; Qu, L.; Lei, Y. Non-destructive Analysis and Deterioration Study of a Decorated *Famille Rose* Porcelain Bowl of Qianlong Reign from the Forbidden City. *Stud. Conserv.* **2019**, *64*, 311–322. [[CrossRef](#)]
85. Molera, J.; Climent-Font, A.; Garcia, G.; Pradell, T.; Vallcorba, O.; Zucchiatti, A. A study of historical processing of cobalt arsenides in XV–XVI century Europe. *J. Archaeol. Sci. Rep.* **2021**, *36*, 102797. [[CrossRef](#)]
86. Zlamalova Cilova, Z.; Gelnar, M.; Randakova, S. Smalt production in the ore mountains: Characterization of samples related to the production of blue pigment in Bohemia. *Archaeometry* **2020**, *62*, 1202–1215. [[CrossRef](#)]
87. Mimoso, J.M. Origin, early history and technology of the blue pigment in azulejos. In Proceedings of the GlazeArch2015, Lisbon, Portugal, 2–3 July 2015; pp. 357–376. Available online: http://azulejos.lnec.pt/AzuRe/links/07%20Origin_of_blue_pigment.pdf (accessed on 20 January 2021).
88. Bunney, M. A new Technique to Help Identify Chinese Ceramic Fakes: Shirley, M. Mueller Interviews. *Am. Ceram. Circ. Spring Newlett.* **2016**, 25–26.
89. Wallace, S.C.; Kenney-Wallace, G. Bubble signatures revealed in antique artefacts. *Phys. World* **2016**, *29*, 34. [[CrossRef](#)]
90. Kirmızı, B.; Chen, S.; Colomban, P. The Raman signature of protonic species as a potential tool for dating or authentication of glazed pottery. *J. Raman Spectrosc.* **2019**, *50*, 696–710. [[CrossRef](#)]
91. Colomban, P.; Treppoz, F. Identification and Differentiation of Ancient and Modern European Porcelains by Raman Macro- and Microspectroscopy. *J. Raman Spectrosc.* **2001**, *32*, 93–102. [[CrossRef](#)]
92. Colomban, P. Polymerization degree and Raman identification of ancient glasses used for jewellery, ceramic enamels and mosaics. *J. Non-Cryst. Solids* **2003**, *323*, 180–187. [[CrossRef](#)]
93. Colomban, P.; Tournié, A.; Bellot-Gurlet, L. Raman identification of glassy silicates used in ceramic, glass and jewellery: A tentative differentiation guide. *J. Raman Spectrosc.* **2006**, *37*, 841–852. [[CrossRef](#)]
94. Yap, C.T.; Tang, S.M. X-ray fluorescence analysis of modern and recent Chinese porcelains. *Archaeometry* **1984**, *26*, 78–81. [[CrossRef](#)]

95. Yap, C.T. A quantitative spectrometric analysis of trace concentrations of manganese and cobalt in ceramics and the significance of As/Co and Mn/Co ratios. *J. Archaeol. Sci.* **1988**, *15*, 173–177. [[CrossRef](#)]
96. Yu, K.N.; Miao, J.M. Locating the origins of blue and white porcelains using EDXRF. *Appl. Radiat. Isot.* **1997**, *48*, 959–963. [[CrossRef](#)]
97. Yu, K.N.; Miao, J.M. Multivariate analysis of the energy dispersive X-ray fluorescence results from blue and white Chinese porcelains. *Archaeometry* **1998**, *40*, 331–339. [[CrossRef](#)]
98. Yu, K.N.; Miao, J.M. Characterization of blue and white porcelains using Mn/Fe ratio from EDXRF, with particular reference to porcelains of the Xuande period (1426 to 1435 A.D.). *Appl. Radiat. Isot.* **1999**, *51*, 279–283. [[CrossRef](#)]
99. Morimoto, A.; Yamasaki, K. *Technical Studies on Ancient Ceramics Found in North and Central Vietnam*; Fukuoka Museum: Fukuoka, Japan, 2001.
100. Cheng, H.S.; Zhang, B.; Xia, H.N.; Jiang, J.C.; Yang, F.J. Non-destructive analysis and appraisal of ancient Chinese porcelain by PIXE. *Nucl. Instr. Meth. Phys. Res. Sect. B* **2002**, *190*, 488–491. [[CrossRef](#)]
101. Zhang, F. The origin and development of traditional Chinese glazes and decorative ceramics color. In *Ancient Technology to Modern Science*; Kingery, W.D., Ed.; The American Ceramic Society: Columbus, OH, USA, 1985; Volume 1, pp. 163–180.
102. Aimé-Martin, M.L. (Ed.) Letter of the Father Dentrecolles, Dated 1 September 1712 + Letter of Father Dentrecolles Dated 25 January 1722. In *Lettres Édifiantes et Curieuses Concernant l'Asie, l'Afrique et l'Amérique, Avec Quelques Relations Nouvelles de Missions et des Notes Géographiques et Historiques*; T. III Chine; Société du Panthéon Littéraire: Paris, France, 1843; pp. 216–233+318–325.s.